MECHANICAL PERFORMANCE OF COMPACTED SLUDGE-CRUSHED SALT MIXTURES AS SEALING MATERIALS IN SALT MINES

Pongpoj Sattra

A Thesis Submitted in Partial Fulfillment of the Requirements for the Degree of Master of Engineering in Geotechnology

Suranaree University of Technology

Academic Year 2016

ศักยภาพเชิงกลศาสตร์ของเกลือบดผสมดินตะกอนประปาสำหรับเป็นวัสดุอุด ในเหมืองเกลือ

นายพงษ์พจน์ สาตรา

วิทยานิพนธ์นี้เป็นส่วนหนึ่งของการศึกษาตามหลักสูตรปริญญาวิศวกรรมศาสตรมหาบัณฑิต
สาขาวิชาเทคโนโลยีธรณี
มหาวิทยาลัยเทคโนโลยีสุรนารี
ปีการศึกษา 2559

MECHANICAL PERFORMANCE OF COMPACTED SLUDGE-CRUSHED SALT MIXTURES AS SEALING MATERIALS IN SALT MINES

Suranaree University of Technology has approved this thesis submitted in partial fulfillment of the requirements for a Master's Degree.

Thesis Examining Committee

(Asst. Prof. Dr. Decho Phueakphum)
Chairperson

(Dr. Prachya Tepnarong)
Member (Thesis Advisor)

(Prof. Dr. Kittitep Fuenkajorn)
Member

(Prof. Dr. Sukit Limpijumnong)
Vice Rector for Academic Affairs and Innovation

(Assoc. Prof . Flt. Lt. Dr. Kontorn Chamniprasart)
Dean of Institute of Engineering

พงษ์พจน์ สาตรา : ศักยภาพเชิงกลศาสตร์ของเกลือบดผสมดินตะกอนประปาสำหรับเป็นวัสดุอุดในเหมืองเกลือ (MECHANICAL PERFORMANCE OF COMPACTED SLUDGE-CRUSHED SALT MIXTURES AS SEALING MATERIALS IN SALT MINES) อาจารย์ที่ปรึกษา : อาจารย์ ดร.ปรัชญา เทพณรงค์, 84 หน้า.

วัตถุประสงค์ของการศึกษานี้คือ เพื่อทดลองประเมินศักยภาพเชิงกลศาสตร์และชลศาสตร์ของส่วนผสมบดอัดดินตะกอนประปาและเกลือบดเพื่อใช้เป็นวัสดุอุด เกลือบดจัดเตรียมจากชั้นเกลือหินชุดมหาสารคามชั้นล่างจากแอ่งโคราชในภาคตะวันออกเฉียงเหนือของประเทศไทย ซึ่งมีขนาดเส้นผ่านศูนย์กลางขนาด 0.075 – 2.35 เซนติเมตร นำมาผสมกับดินตะกอนประปาจากการประปานครหลวงแห่งประเทศไทย (กปน.) โดยมีอัตราส่วนของตะกอนประปาผสมกับเกลือบด 10:90, 20:80, 30:70, 40:60, 50:50, 60:40, 70:30, 80:20, 90:10 และ 100:0 การทดสอบบดอัดถูกดำเนินการเพื่อคำนวณหาปริมาณน้ำเกลอที่เหมาะสม การทดสอบกำลังรับแรงเฉือนโดยตรงถูกดำเนินการเพื่อหาความต้านทานแรงเฉือนของส่วนผสม การทดสอบค่าความซึมผ่านถูกกำหนดเพื่อหาค่าความซึมผ่านแท้จริงของตัวอย่างหลังการบดอัด การจำลองทางคอมพิวเตอร์ได้ถูกใช้เพื่อตรวจสอบประสิทธิภาพของวัสดุผสมเพื่อเป็นวัสดุถมกลับในเหมืองเกลือหลังการขุดเจาะสำเร็จไปแล้ว อัตราส่วนดินตะกอนประปาต่อเกลือบด 20:80 เป็นอัตราส่วนที่ดีที่สุดในการศึกษานี้สำหรับใช้เป็นวัสดุถมกลับเพราะอัตราส่วนนี้ให้ค่าคุณสมบัติทางกลศาสตร์มากที่สุดสำหรับการค้ำยันเสาในเหมืองเกลือ

สาขาวิชา เทคโนโลยีธรณี ลายมือชื่อนักศึกษา_____

ปีการศึกษา 2559 ลายมือชื่ออาจารย์ที่ปรึกษา_____

PONGPOJ SATTRA : MECHANICAL PERFORMANCE OF COMPACTED SLUDGE-CRUSHED SALT MIXTURES AS SEALING MATERIALS IN SALT MINES. THESIS ADVISOR : PRACHYA TEPNARONG, Ph.D., 84 PP.

COMPACTION/SLUDGE/CRUSHED SALT/SEALING MATERIALS

The objective of this study is to experimentally assess the mechanical and hydraulic performance of compacted sludge-crushed salt for use as the sealing materials. Crushed salt is prepared from the Lower Members of the Maha Sarakham Formation in the Korat basin, northeastern Thailand. It has size ranges from 0.075 to 2.35 mm diameters. They are mixed with the sludge obtained from the Metropolitan Waterworks Authority of Thailand (MWA). The percentage weight ratios of the sludge-crushed salt specimens are 10:90, 20:80, 30:70, 40:60, 50:50, 60:40, 70:30, 80:20, 10:90 and 100:0. The compaction tests are performed to determine the optimum brine content. The direct shear tests are conducted to determine the shearing resistance of the mixtures. The permeability testing is performed to determine intrinsic permeability of the mixtures after the compaction. The computer simulation is used to determine the effectiveness of backfill in salt mines after the mine excavation completed. The sludge to crushed salt 20:80 ratio is probably the best ratio for backfill in this study because this ratio gives the maximum mechanical properties for supporting pillar in salt mine.

School of Geotechnology Student's Signature_____

Academic Year 2016 Advisor's Signature_____

ACKNOWLEDGMENTS

I wish to acknowledge the funding supported by Suranaree University of Technology (SUT).

I would like to express my sincere thanks to Dr. Prachya Tepnarong for his valuable guidance and efficient supervision. I appreciate his strong support, encouragement, suggestions and comments during the research period. My heartiness thanks to Prof. Dr. Kittitep Fuenkajorn and Asst. Prof. Dr. Decho Phueakphum for their constructive advice, valuable suggestions and comments on my research works as thesis committee members. Grateful thanks are given to all staffs of Geomechanics Research Unit, Institute of Engineering who supported my work.

Finally, I would like to thank beloved parents for their love, support and encouragement.

Pongpoj Sattra

TABLE OF CONTENTS

Page

TABLE OF CONTENTS (Continued)

Page

TABLE OF CONTENTS (Continued)

Page

LIST OF TABLES

Table **Page**

LIST OF TABLES (Continued)

Page

LIST OF FIGURES

Figure **Page**

LIST OF FIGURES (Continued)

Figure **Page**

LIST OF FIGURES (Continued)

Figure **Page**

LIST OF FIGURES (Continued)

Figure **Page**

LIST OF FIGURES (Continued)

Figure **Page**

SYMBOLS AND ABBREVIATIONS

ρ	=	Density
μ	=	Dynamic viscosity of fluid
γ	=	Unit weight of fluid
c	=	Cohesion
ϕ	=	Friction angle
σ_n	=	Normal stress
τ	=	Shear stress
e	=	Void ratio
k	=	Intrinsic permeability
K	=	Coefficient of permeability
Q	=	Flow rate
ν	=	Poisson's ratio
σ_c	=	Uniaxial compressive strengths
Δh	=	Head different
ΔL	=	Length changes over time
W_B	=	Brine content

CHAPTER I

INTRODUCTION

1.1 Background and Rationale

Sealing material is one of the key to reduce the environmental impacts induced by underground minings, including surface subsidence and salinity of the nearby farmlands and surface water. A common solution practiced internationally in the mining industry is to use bentonite-crushed salt as a sealing material. The bentonite is, however, expensive and can be highly consolidated even under low loading. Alternative materials, such as sludge, is of interest for use to mix with the waste crushed salt due to their suitable hydraulic and mechanical properties. Sludge is the waste material obtained from the water treatment plant. The mixture is intended for use as sealing material in salt and potash mines.

1.2 Research objectives

The objective of this study is to experimentally determine the mechanical and hydraulic performance of compacted sludge and crushed salt with saturated brine. The three-ring compaction mold which is developed by Sonsakul and Fuenkajorn (2013) is used to perform compaction test, direct shear test on various ratios of the sludge and crushed salt mixtures. FLAC 4.0 model is used to simulate the opening deformability and surface subsidence before and after backfilling. The findings can be useful to design the sealing material for opening in salt and potash mines.

1.3 Scope and Limitations

1) Sludge is obtained from Metropolitan Waterworks Authority with grain sizes ranging from 0.075 to 0.475 mm.
2) Crushed salt is prepared from the Maha Sarakham formation, which has grain size ranging from 0.075 to 2.35 mm.
3) Basic characterization tests are performed, including the compaction test, direct shear test and permeability test. The test procedures are followed the relevant ASTM standard practices.
4) The applied normal stresses for the direct shear vary from 0.05, 0.1, 0.2, 0.4 to 0.6 MPa.
5) Up to 25 samples are tested.
6) Compaction and direct shear testing is performed by three-ring mold (Sonsakul and Fuenkajorn ., 2013).
7) Permeability test is performed by constant head test method, which constant head is at 120 cm.
8) FLAC 4.0 is used to study the salt mine deformation. The overburden thickness is assumed as 100, 150 and 200 m. The opening height are 2, 4 and 6 m. The opening width is 8 m.

1.4 Research methodology

1.4.1 Literature review

Literature review is carried out to study the sludge useful and the relevant theory of compaction test, direct shear test and permeability test. The sources

of information are from text books, journals, technical reports and conference papers. A summary of the literature review is given in the thesis.

1.4.2 Sample preparation

Sludge is collected from the Metropolitan Waterworks Authority and passing sieve number 40, Rock salt is obtained from the Asean Potash Mining Public Company Limited at Bamnet Narong district, Chaiyaphum province and is crushed in machine until they can pass sieve number 4. Saturated brine is prepared from pure salt (NaCl) of 2.7 kg with distilled water in plastic tank and stirred by a plastic stick continuously for 20 minutes. The proportion of salt and water is more than 39% by weight.

1.4.3 Compaction Test

Sludge and crushed salt mixture ratio (S:C) 100:0, 90:10, 80:20, 70:30, 60:40, 50:50, 40:60, 30:70, 20:80 and 10:90 are mixed with the saturated brine with percentages of mixture of 0, 5, 10, 15, 20, 25, 30, 35 and 40%. The mixtures are compacted in the three-ring mold to determine the optimum brine content and maximum dry density

1.4.4 Direct Shear Test

The direct shear test is performed to determine maximum shear stresses of the mixtures by using three-ring mold. The normal and shear force are applied by the hydraulic load cell. Normal stresses used here are 0.05, 0.1, 0.2, 0.4 and 0.6 MPa for the three-ring mold. The peak shear strength is used to calculate the cohesion and friction angle.

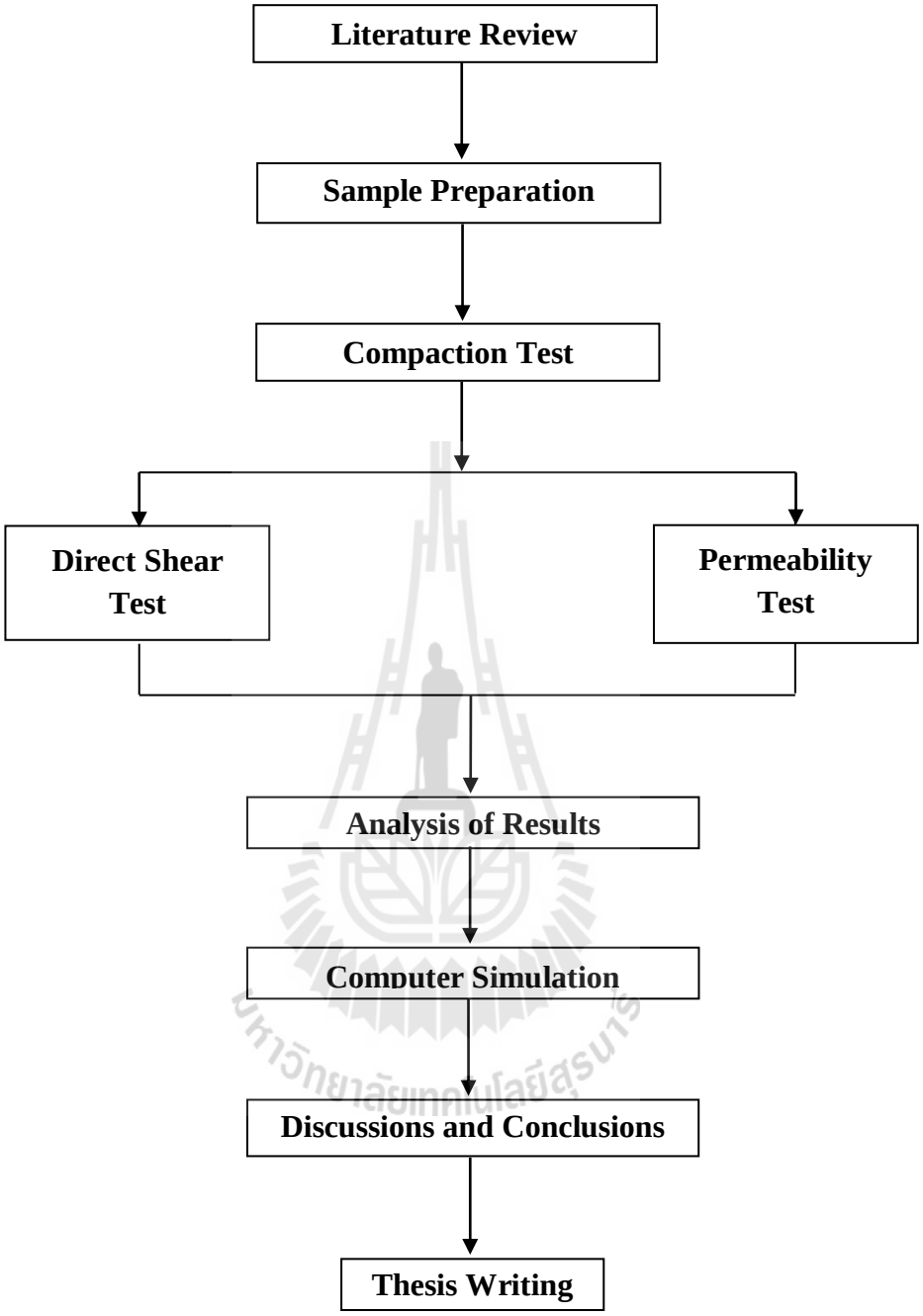

Figure 1.1 Study plan

1.4.5 Permeability Test

The flow testing is performed to determine intrinsic permeability of sludge-crushed salt mixtures by the constant head test method. The test results are used to select an appropriate ratio of the mixtures. The samples from the compaction mold are put into a PVC pipe of 10.16 cm diameter and 16.52 cm height.

1.4.6 Analysis of Results

The direct shear tests with various normal stresses is used to determine the cohesion (c) and friction angle (ϕ) by using Mohr-Coulomb failure criterion. The effect of the sludge-crushed salt ratios by weight is determined in terms of permeability and shear strength.

1.4.7 Computer simulation

Finite difference method (FLAC 4.0) are used to simulate effect of backfill material in salt and potash mines under the conditions with various overburden thickness, time before backfill, room height and percent of compacted sludge-crushed salt.

1.4.8 Discussions and Conclusion

Results from laboratory testing are used to analyze sealing performance of compacted sludge-crushed salt in terms of the mechanical and hydraulic properties for applications in the fields.

1.4.9 Thesis Writing

All research activities, methods, and results will be documented and complied in the thesis. This research is application to design mine sealing which soil strength parameter of direct shear test. The findings are published in the conference proceedings or journals.

1.5 Thesis contents

Chapter I states the objectives, rationale, and methodology of the research. **Chapter II** summarizes results of the literature review on direct shear and laboratory testing. **Chapter III** describes sample preparation and laboratory test. **Chapter IV** describes the results from the laboratory experiments. The experiments are divided into 3 tests, including 1) compaction tests 2) direct shear testing and 3) permeability test. **Chapter V** shows result of surface subsidence which simulated by using computer simulation (FLAC) **Chapter VI** discusses and concludes the research results, and provides recommendations for future research studies.

CHAPTER II

LITERATURE REVIEW

2.1 Introduction

Relevant topics and previous research results are reviewed to improve an understanding basic properties of sludge, compaction test, direct shear test, ASTM standard properties of these test and computer modelling. The initial review results are summarized below.

2.2 Basic properties of sludge

Valls et al. (2004) study the sludge mixed with Portland cement. The specimens of concrete contain different percentages of sludge from a sewage treatment plant. Both physical properties (density, porosity, and absorption capacity) and mechanical properties (compressive strength, flexural strength, and elastic modulus) are studied. The results confirm that up to 10% of treatment plant sludge can be added to concrete for use in certain very specific applications.

Wetchasat and Fuenkajorn (2013) study the performance of sludge mixed with the commercial grade Portland cement type I for use in reducing permeability of fractures in sandstone. The fractures are artificially made in Phu Kradung sandstone by applying a line load to induce a splitting tensile crack in 0.15x0.15x0.15 m prismatic blocks. The Bang Khen water treatment sludge is used. More than 80% of the sludge is quartz with grain size less than 75 μm liquid limit 55 plastic limit 22

plasticity index 23 and specific gravity 2.56. The results indicate that the suitable mixing ratios for sludge:cement (S:C) are 1:10, 3:10, 5:10 with water-cement ratio (W:C) of 1:1 by weight. These proportions yield the lowest slurry viscosity of 5 Pa·s. For S:C = 3:10, the compressive strength and elastic modulus are 1.22 and 224 MPa which are similar to those of bentonite mixed with cement. The shear strength of grouted fractures varies from 0.22 to 0.90 MPa under normal stresses ranging from 0.25 to 1.25 MPa. Permeability of grouting materials is from 10^{-17} to 10^{-15} m^2 and decreases with curing time. The S:C ratio of 5:10 gives the lowest permeability. Permeability of grouted fractures with apertures of 2, 10 and 20 mm range from 10^{-16} to 10^{-14} m^2.

Gullu and Girisken (2013) study the performance of fine-grained soil treated with industrial wastewater sludge. The experimental program conducts the standard compaction, direct shear, California bearing ratio (CBR), and unconfined compressive strength (UCS) tests. The sludge proportions in samples of the soil-sludge mixtures are 0, 5, 10, 20, 30, 40, 50, 60, 70, and 80 % by dry weight of the mixture. The results indicate that the internal friction angle of untreated soil is significantly enhanced at most of the sludge dosages. The CBR values offer that the soil quality can be improved to good rating quality to use base layers in stabilizations up to the 50 % sludge dosage. The contribution is also obtained by the UCS values that increase with the sludge addition. Moreover, the stress–strain responses promise to develop the ductility behavior due to the sludge inclusion. Consequently, the soil mixtures treated with the sludge have exhibited satisfactory geotechnical characteristics. Thus, this study suggests that the industrial wastewater sludge can be potentially employed for improvement of fine-grained soil in the stabilizations. The proposed soil stabilization

with locally available industrial wastewater sludge can also provide recycling and sustainability to the environment.

2.3 Compaction Test.

ASTM (D1557) determines the relationship between the moisture content and the dry density of a soil for a specified compactive effort. The compactive effort is the amount of mechanical energy that is applied to the soil mass. Several different methods are used to compact soil in the field, and some examples include tamping, kneading, vibration, and static load compaction. This laboratory employs the tamping or impact compaction method using the type of equipment and methodology developed by R. R. Proctor (1933), therefore, the test is also known as the Proctor test. Two types of compaction tests are routinely performed: (1) the Standard Proctor test, and (2) the Modified Proctor test. Each of these tests can be performed in three different methods as outlined in the attached Table 1. In the Standard Proctor test, the soil is compacted by a 5.5 lbs hammer falling a distance of one foot into a soil filled mold. The mold is filled with three equal layers of soil, and each layer is subjected to 25 drops of the hammer. The Modified Proctor test is identical to the Standard Proctor test except it employs, a 10 lbs hammer falling a distance of 18 inches, and uses five equal layers of soil instead of three. There are two types of compaction molds used for testing. The smaller type is 4 inches in diameter and has a volume of about 1/30 ft^3 (944 cm^3), and the larger type is 6 inches in diameter and has a volume of about 1/13.333 ft^3 (2,123 cm^3).

If the larger mold is used each soil layer must receive 56 blows instead of 25 (Table 2.1). Mechanical compaction is one of the most common and cost effective

means of stabilizing soils. An extremely important task of geotechnical engineers is the performance and analysis of field control tests to assure that compacted fills are meeting the prescribed design specifications. Design specifications usually state the required density, and the water content.

Table 2.1 Alternative Proctor Methods (Reddy, 2005)

	Standard Proctor ASTM 698			Modified Proctor ASTM 1557		
	Method A	Method B	Method C	Method A	Method B	Method C
Material	≤ 20% Retained on No.4 Sieve	>20% Retained on No.4 ≤ 20% Retained on 3/8"Sieve	>20% Retained on No.3/8" <30% Retained on 3/4"Sieve	≤ 20% Retained on No.4 Sieve	>20% Retained on No.4 ≤ 20% Retained on 3/8"Sieve	>20% Retained on No.3/8" <30% Retained on 3/4"Sieve
For test sample, use soil passing	SieveNo.4	3/8"Sieve	3/4"Sieve	SieveNo.4	3/8"Sieve	3/4"Sieve
Mold	4" DIA	4" DIA	6" DIA	4" DIA	4" DIA	6" DIA
No. of layers	3	3	3	5	5	5
No. of blows/layer	25	25	56	25	25	56

Note: Volume of 4" diameter mold = 944 cm^3, Volume of 6" diameter mold = 2123 cm^3 (verify these values prior to testing)

In general, most engineering properties, such as the strength, stiffness, resistance to shrinkage, and imperviousness of the soil, will improve by increasing the soil density. The optimum water content is the water content that results in the greatest density for a specified compactive effort. Compacting at water contents higher than

(wet of) the optimum water content results in a relatively dispersed soil structure (parallel particle orientations) that is weaker, more ductile, less pervious, softer, more susceptible to shrinking, and less susceptible to swelling than soil compacted dry of optimum to the same density. The soil compacted lower than (dry of) the optimum water content typically results in a flocculated soil structure (random particle orientations) that has the opposite characteristics of the soil compacted wet of the optimum water content.

Ran and Daemen (1995) study the dynamic compaction tests of bentonite-based materials. The results of laboratory compaction testing to determine the influence of particle size, size gradation and moisture content on compaction of crushed rock salt. Included is a theoretical analysis of the optimum size gradation. The results indicate that compaction increases with maximum particle size and compaction energy, and varies with particle size gradation and water content until the optimum water content is reached (5%), and decreases with further water content increases (Figure 2.1).

Hansen (1997) conducts brine permeability and mechanical properties on dynamically compacted crushed salt in the Waste Isolation Pilot Plant (WIPP) shafts. The results from brine permeability test indicate that the apparent permeability is found to decrease from initial value of about 5×10^{-16} m^2 to 0 flows after 10 days. The mechanical results include axial, radial, and volumetric creep strains as a function of time. The figure 2.2 show the creep strains for sample RS/DCCS/1, tested under shear consolidation conditions of σ_1 = 5 MPa and σ_3 = 1 MPa.

2.4 Direct Shear Test

Das (2008) states that the direct shear method is the oldest and simplest form of shear test arrangement. A diagram of the direct shear test apparatus is shown in figure 2.3 the test equipment consists of a metal shear box in which the soil specimens may be square or circular. The size of the specimens used is about 3 to 4 in2 across 1 in high. Normal force on the specimen is applied from the top of shear box. The normal stress on the specimens can be as 150 psi. Shear force is applied by moving one half of the box relative to the other to cause failure in the soil specimen. Depending on equipment, the shear test can be either stress-controlled or strain-controlled. In stress-controlled tests, the shear force is applied in equal increments until the specimen fails. The failure takes place along the plane of split of shear box. After the application of each incremental load, the shear displacement of the top half of the box is measured by a horizontal dial gauge. The change in the height of the specimen (and thus the volume change of the specimen) during the test can be obtained from the reading of the dial gauge that measures the vertical movement of the upper loading plate. In stain-controlled tests, a constant rate of shear displacement is applied to one half of the box by a motor that act through gears. The constant rate of shear displacement is measured by a horizontal dial gauge. The resisting shear force of the soil corresponding to any shear displacement can be measured by a horizontal proving ring or load cell.

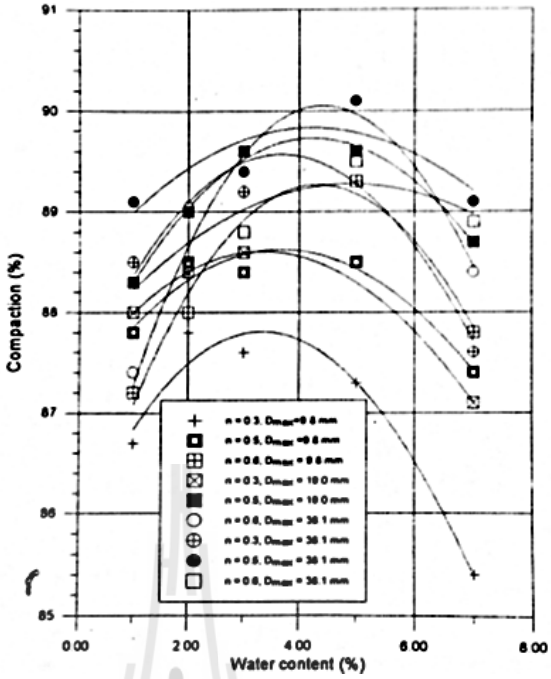

Figure 2.1 Compaction as a function of water content and particle size gradation (Ran and Daemen, 1995).

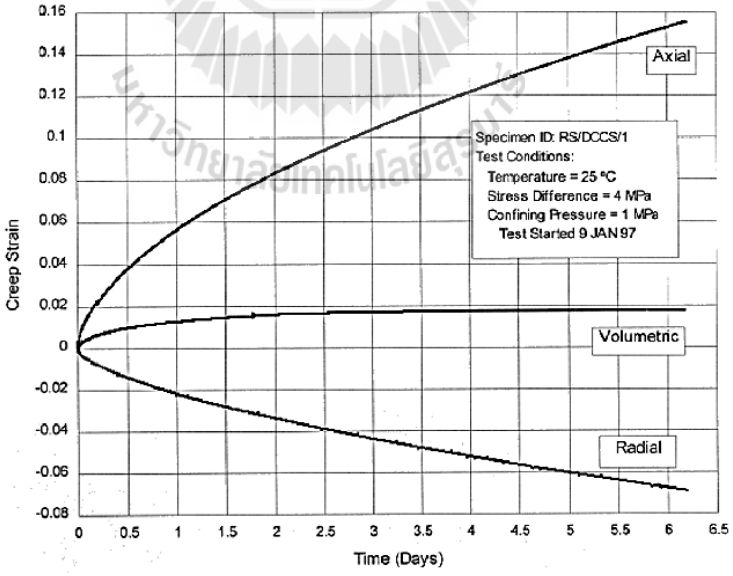

Figure 2.2 Shear consolidations at a mean stress of 2.33 MPa (Hansen, 1997).

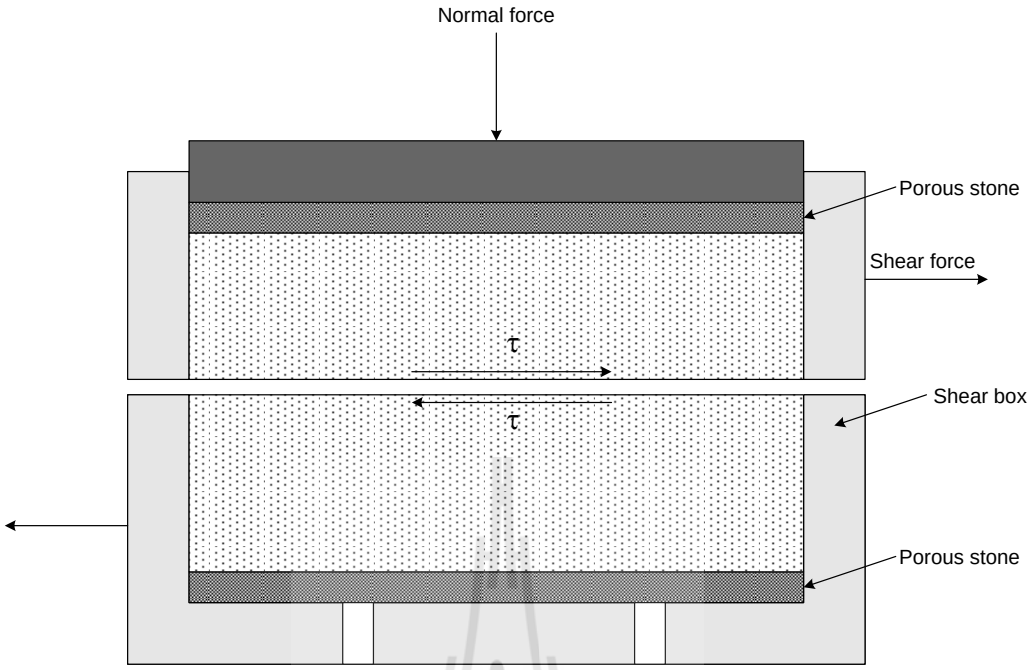

Figure 2.3 Diagram of direct shear test arrangement (Das, 2008).

The volume change of the specimen during the test is obtained in a manner similar to the stress-controlled test.

Sonsakul, et al. (2013) develop three-ring compaction and direct shear mold. It has been developed to obtain the optimum water content dry density and shear strength of compacted soil samples. The device can shear the soil samples with grain size up to 10 mm. It can be used as a compaction mold and direct shear mold without removing the soil sample, and hence eliminating the sample disturbance. Commercial grade bentonite is tested to verify that the three-ring mold can provide the results comparable to those obtained from the ASTM standard testing devices. Three types of soil, including clayey sand, poorly-graded sand and well-graded sand, are tested to assess the performance of the device. Their results are compared with those obtained from the ASTM standard test device. The results indicate that the shear strength, maximum

dry density and optimum water content of the bentonite obtained from the three-ring mold and the ASTM standard mold are virtually identical. The three-ring mold yields the higher maximum dry density than those obtained from the standard mold. The shear strengths obtained from the three-ring mod are also higher than those from the standard shear test device. This is primarily because the three-ring mold can accommodate the soil particles up to 10 mm for the shear test, and hence resulting in higher shear strengths that are closer to the actual behavior of the soil under in-situ conditions.

2.5 Laboratory Test

ASTM (D422) determines the percentage of different grain sizes contained within a soil. The mechanical or sieve analysis is performed to determine the distribution of the coarser, larger-sized particles, and the hydrometer method is used to determine the distribution of the finer particles. The distribution of different grain sizes affects the engineering properties of soil. Grain size analysis provides the grain size distribution, and it is required in classifying the soil.

ASTM (D854-00) determines the specific gravity of soil by using a pycnometer. Specific gravity is the ratio of the mass of unit volume of soil at a stated temperature to the mass of the same volume of gas-free distilled water at a stated temperature. The specific gravity of a soil is used in the phase relationship of air, water, and solids in a given volume of the soil.

ASTM (D5856-15) determines the hydraulic conductivity (also referred to as coefficient of permeability) of laboratory compacted materials.

Hydraulic conductivity is the rate of discharge of water under laminar flow conditions through a unit cross-sectional area of porous medium under a unit hydraulic gradient and standard temperature conditions (20° C)

Kelsall et al. (1984) propose to use crushed salt as a major backfill component in schematic designs for penetration seal for salt repositories. Creep closure of the storage room, tunnels, and shafts is likely to compress the crushed salt backfill and create an impermeable monolith to retard ground water flow and radionuclide migration.

Case and Kelsall (1987) study the potential of crushed for required sealing access shafts and drifts for long periods. Crushed salt backfill is being investigated as a potential backfill and seal material through laboratory testing to determine how fundamental properties such as permeability, porosity and creep rate are reduced by pressure and time through consolidation. The test program reported in this paper consisted of four consolidation tests using crushed salt obtained from the Waste Isolation Pilot Plant and the Avery Island Mine. Tests with one- or two-month durations were conducted on samples with maximum particle sizes of 1, 10, and 20 mm, with initial porosities ranging from 26 to 36%, moisture contents of zero and 2%, and initial permeability from 10^3 to 10^5 m^2. The tests were performed at ambient temperature and confining pressures ranging from 0.34 MPa to 17 MPa. The most significant observation from the tests was the influence of moisture on changes in permeability, porosity and volumetric creep strain rate. The final permeability and porosity of one moist sample were reduced after one month to about 10^{-5} m^2 and 5%, respectively, compared to about 10^{-2} m^2 and 14 to 19% for the dry samples. In addition, the consolidation rate for the moist sample was more rapid at comparable

porosities. In all of the tests, the volumetric creep strain rate tanged from 10^{-8} to 10^{-6} /sec, and did not achieve steady state values after 1 to 2 months of load application.

Fuenkajorn and Daemen (1987) study the mechanical relationship between cement, bentonite and surrounding rock. The study deals with the mechanical interaction between multiple plugs and surrounding rock and identification of potential failure. Two conceptual plug designs are studied. Pipe tests have been performed to determine the swelling pressures of 60 mm diameter bentonite plugs and of 64 mm diameter cement plugs. The axial and radial swelling pressures of a bentonite plug specimen are 7.5 and 2.6 MPa after adsorbing water for 5 days. The maximum radial expansive stresses of the cement plugs cured for 25 days are 4.7 and 2.7 MPa for system 1 and system 3 cements. Results from the experiment indicate that in order to obtain sufficient mechanical stability of bentonite seal, the sealing should be done below groundwater level. If cement material is used to seal in hard rock, the mechanical stability will be higher than sealing in soft rock.

Butcher (1991) concluded that a 70% by weight salt and 30 % by weight bentonite mixture is preferable to pure crushed salt as backfill for disposal rooms in the Waste Isolation Pilot Plant. The performance of two backfill materials is examined with regard to various selection criteria related to compliance with transuranic radioactive waste standard 40 CFR 191, Subpart B, such as the need for low liquid permeability after closure, chemical stability, strength, ease of emplacement, and sorption potential for brine and radionuclides. Both salt and salt/bentonite are expected to consolidate to a final state of permeability $\leq 10^{-18}$ m^2, which is adequate for satisfying government regulations for nuclear repositories. The real advantage of the salt/bentonite backfill depends, therefore, on bentonite's potential for absorbing

brine and radionuclides. Estimates of the impact of these properties on backfill performance are presented.

Hansen (1997) study the dynamic compacted crushed salt. The material has the moisture contents of 1.6 % by weight. The test procedures included shear consolidation, constant strain rate and permeability tests. The figure 2.4 shows volumetric strain as a function of time on the primary axis and brine flow as a function of time on the secondary axis. Permeability testing of the dynamically compacted crushed salt provided further evidence that the permeability decrease as the fraction density of the salt increases. The model predicted that stress states exist where the radial strain rate would initially be positive (consolidation) and then reverse direction and become negative as the specimen density increases.

2.6 Numerical simulations

FLAC developed by Itasca Consulting Group Inc. (1992). FLAC is a two-dimensional explicit finite difference program for engineering mechanics computation. This program simulates the behavior of structures built of soil, rock, or other materials that may undergo plastic flow when their yield limits are reached. Materials are represented by elements, or zones, that form a grid that is adjusted by the user to fit the shape of the object to be modeled. The Department of mineral Resource classified and interpreted data of salt and potash in northeastern Thailand for study and compare the total boreholes which had been drilled as many as 194 drill holes from 1973 to 1982.

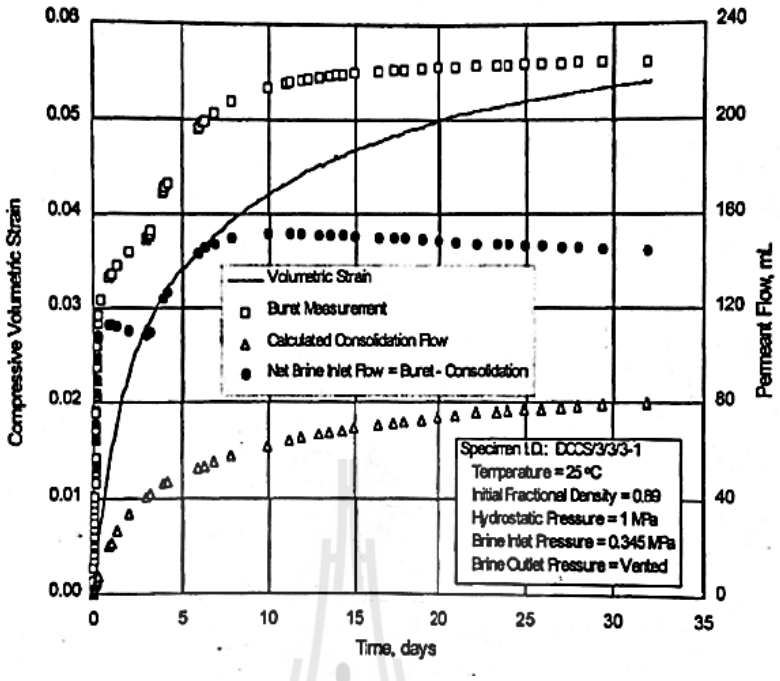

Figure 2.4 Volumetric strain and brine flow as function of time (Hansen and Mellegard, 1997).

The result show rock strata of Maha Sarakham Formation which mostly composed of rock salt can be divided under the overburden or top soil as, Upper Clastic, Upper salt, Middle Clastic, Middle salt, Lower Clastic, Coloured Salt, Potash Zone, Lower Salt, Basal Anhydrite and some minor other layers

CHAPTER III

SAMPLE PREPARATIONS

3.1 Introduction

This chapter describes the basic characteristics and preparation of materials tested in the study. Materials used in this study experiment consist of sludge and crushed salt.

3.2 Sample preparations

3.2.1 Sludge

Sludge samples used in this study are obtained by Metropolitan Waterworks Authority. The chemical compositions of sludge are as shown in Table 3.1. Dried sludge is taken out and dehydrated by drying under sunlight. The moisture is removed one more time in a hot-air oven at 100°C for at least 24 hours or until its weight remains constant. The dried sludge is sieved through the mesh number 40 (sieve opening 0.42 mm) to obtain grain size ranging from 0.001 to 0.475 mm (Figure 3.1). The basic properties of sludge indicate that liquid limit is 59%, plastic limit is 31%, plastic index is 28% and specific gravity 2.56. The sludge sample are classified to the Unified Soil Classification System in the MH (Silt)

3.2.2 Crushed salt

Crushed salt (Figure 3.2) used in this study is prepared from the Lower member of the Maha Sarakham formation in the Korat basin, northeastern Thailand.

The salt sample is donated by Asean Potash Mining Co., Ltd. They are crushed by hammer mill (Figure 3.3) (2HP-4 POLES, Spec jis c-4004) to obtain grain size ranging from 0.075 to 2.35 mm. The sieve analysis determines the grain size distribution of the crushed salt (Figure 3.4). The crushed salt is passing through sieve number 4, 8, 18, 40, 60, 100, 140 and 200. Their openings are 4.75, 2.36, 1, 0.425, 0.25, 0.15, 0.106 and 0.075 mm, respectively.

3.2.3 Saturated brine

Saturated brine is prepared from pure salt (NaCl) of 2.7 kg dissolved with distilled water in plastic tank and stirred by a plastic stick continuously for 20 minutes. The proportion of salt and water is more than 39% by weight. The specific gravity of saturated brine can be calculated by $SG_{Brine} = \rho_{Brine}/\rho_{H2O}$, where SG_{Brine} is specific gravity of saturated brine, ρ_{Brine} is density of saturated brine (measured with a hydrometer (kg/m^3)) and ρ_{H2O} is density of water (kg/m^3) equal 1,000 kg/m^3. The SG of the saturated brine in this study is 1.211 at 21°C.

Table 3.1 Chemical compositions of sludge (Wetchasat, 2013).

Chemical composition	Concentration (% weight)
Na_2O	0.22
MgO	0.96
Al_2O_3	23.47
SiO_2	52.37
P_2O_5	0.34
SO_3	0.55
Cl	0.07
K_2O	1.55
CaO	0.79

Chemical compositions	Concentration (% weight)
TiO_2	0.79
V_2O_5	0.02
Cr_2O_3	0.02
MnO	0.22
Fe_2O_3	6.33
CuO	0.01
Rb_2O	0.01
SrO	0.01
Y_2O_3	<0.01
ZrO_2	0.03
Nb_2O_5	<0.01
BaO	0.01
CeO_2	-
LOI. at 1,025 °C	12.20
Total	100

Figure 3.1 Sludge sample.

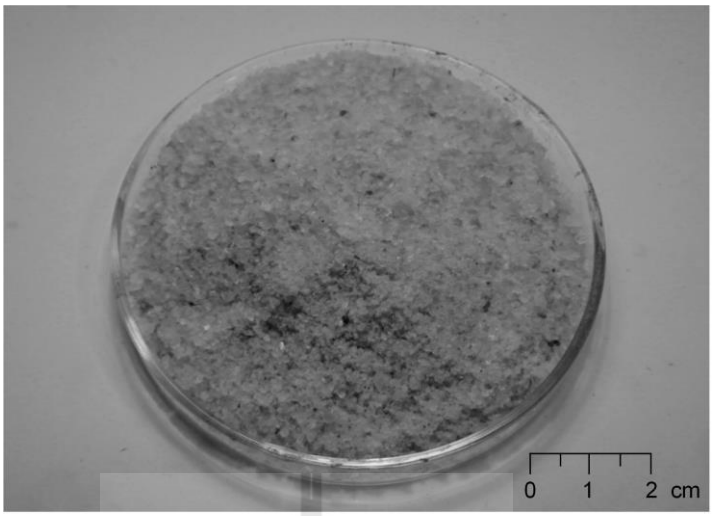

Figure 3.2 Crushed salt sample.

Figure 3.3 Salt sample crushed by hammer mill.

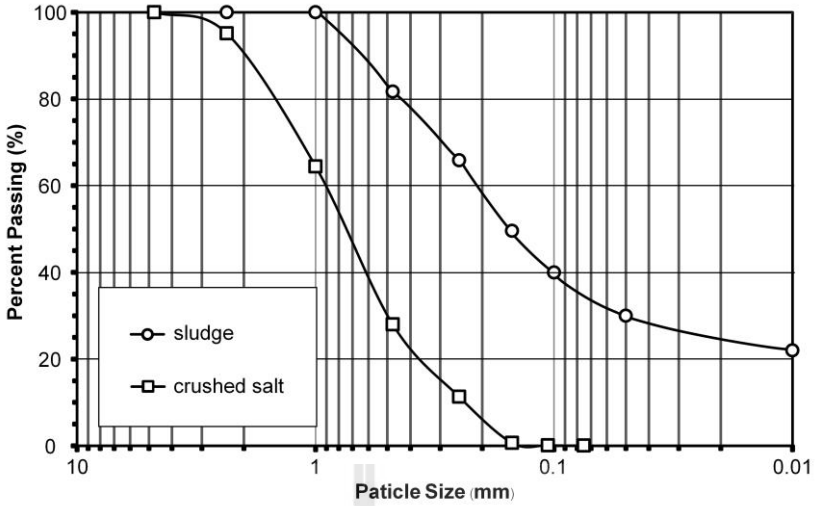

Figure 3.4 Grain size distribution of samples.

CHAPTER IV

LABORATORY TESTING

4.1 Introduction

This chapter describes the test methods and their results obtained from the laboratory experiments to determine the mechanical and hydraulic properties of compacted sludge and crushed salt mixtures.

4.2 Laboratory test

4.2.1 Compaction test

A three-ring compaction mold (Sonsakul and Fuenkajorn, 2013) is used for compaction test and direct shear test, as shown in Figure 4.1. Sludge (S) and crushed salt (C) mixture ratios of 100:0, 90:10, 80:20, 70:30, 60:40, 50:50, 40:60, 30:70, 20:80 and 10:90 by weight are mixed with saturated brine at 0, 5, 10, 15, 20, 25, 30, 35 and 40% by weight to determine the optimum brine content. The mixtures are compacted with a release of weight steel hammer 10 pounds in mold of 27 times per layer in six layers. Energy of compaction can be calculated by (Proctor, 1933):

$$n = \frac{J \times V}{W \times L \times t} \tag{4.1}$$

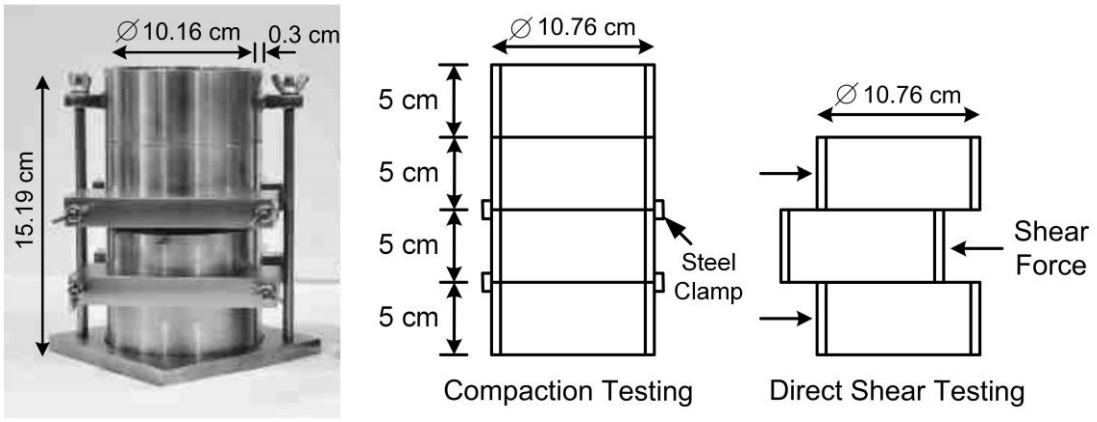

Figure 4.1 Composition of three-ring mold (Sonsakul and Fuengkajorn, 2013)**.**

where J is compaction energy per unit volume, W is weight of hammer, L is height of drop of hammer, t is number of layers, n is number of blows per layer and V is volume of mold. The brine content (W_B) can be calculated by (Fuenkajorn, 1988):

$$W_B = \frac{[100 + S_B] \times [W_1 - W_2 - (\frac{W_i}{100})(W_2 - W_{can})] \times 100}{100 \times (W_2 - W_{can}) - SB(W_1 - W_2)} \quad (4.2)$$

where W_B is brine content (%), W_i is initial water content of specimen (%), W_{can} is weight of container (g), W_1 is weight of wet soil and container (g), W_2 is weight dry soil and container (g) and S_B is solubility of salt in dissolved water (weight crushed salt / weight water) × 100%. The dry densities and brine contents are plotted to determine the maximum dry density and optimum brine content (Figure 4.2). The results show that the maximum dry density decreases with increasing percentages of sludge, and optimum brine content increases with increasing percentage of sludge. Table 4.1 summarizes the results of the compaction test.

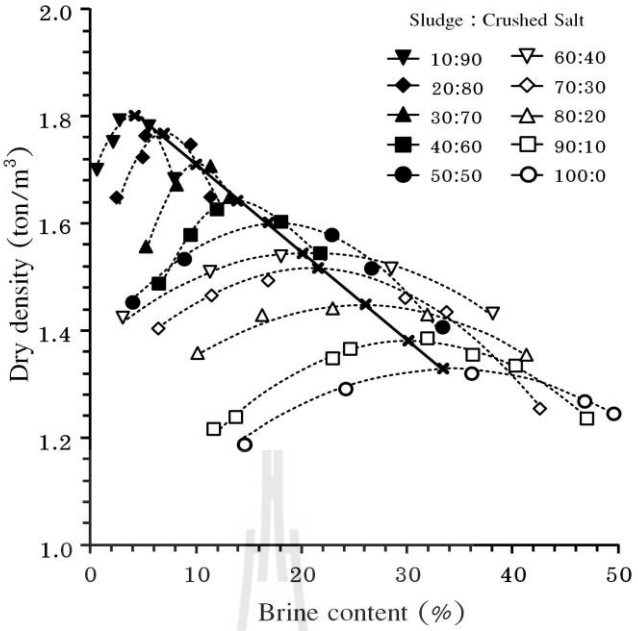

Figure 4.2 Relationship between dry density and brine content as function of sludge content.

Table 4.1 Compaction test results.

Sludge (S) : crushed salt (C)	Optimum brine content (%)	Maximum dry density (ton/m^3)
100:0	34	1.32
90:10	31	1.38
80:20	27	1.44
70:30	23	1.52
60:40	21	1.54
50:50	17	1.60
40:60	14	1.64
30:70	10	1.70
20:80	7	1.76
10:90	4	1.78

4.2.2 Direct shear test

The direct shear test is performed to determine maximum shear strengths of the sludge and crushed salt mixtures with the optimum brine content after compacted in the three ring mold. Figure 4.3(a) shows the direct shear test frame developed for the three-ring mold. The main components for the shear test frame are the lateral load system for pushing the middle ring and the vertical load system for applying a constant normal load on the compacted sample (Figure 4.3(b)). Normal stresses used are 0.05, 0.1, 0.2, 0.4 and 0.6 MPa. The normal and shear force are applied by a hydraulic load cell. The shear stressed is applied while the shear displacement and dilation are observed for every 0.1 mm of shear displacement. The shear and normal stress can calculate from the equation:

$$\tau = F/2A \tag{4.3}$$

$$\sigma_n = P/A \tag{4.4}$$

where τ is the shear stress, F is sheared force, A is cross section area of sample, σ_n is normal stress, P is normal load. The shear stresses as a function of shear displacement are shown in Figure 4.4. The shear stresses increase with shearing displacement, particularly under high normal stresses. The results are shown in the form of the Coulomb's criterion. It can be expressed as:

$$\tau = c + \sigma tan\phi \tag{4.5}$$

where τ and σ are the shear stress and normal stress, ϕ is the angle of internal friction, and c is cohesion. The test results are shown in forms of the shear strength as a

function of normal stress. The peak shear strength is used to calculate the cohesion and friction angle. Figure 4.5 shows peak shear stresses as a function of normal stresses with varying. Figure 4.6 shows friction angle as a function of sludge content and Figure 4.7 shows cohesion as a function of sludge content. Table 4.2 shows the cohesion and friction angle obtained from the direct shear testing. The higher shear strength is obtained from the higher percentages of crushed salt mixtures.

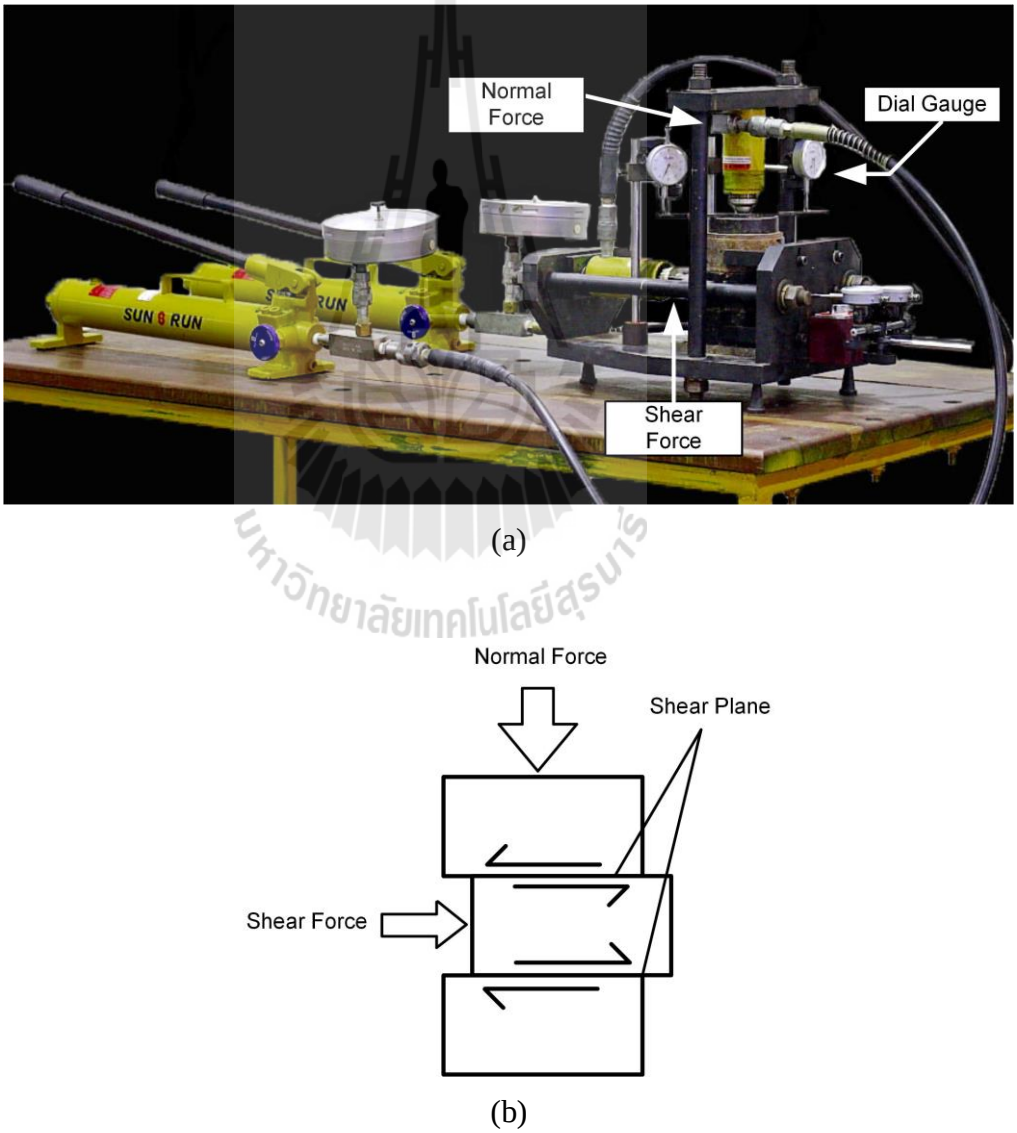

Figure 4.3 Three-ring compaction and direct shear mold.

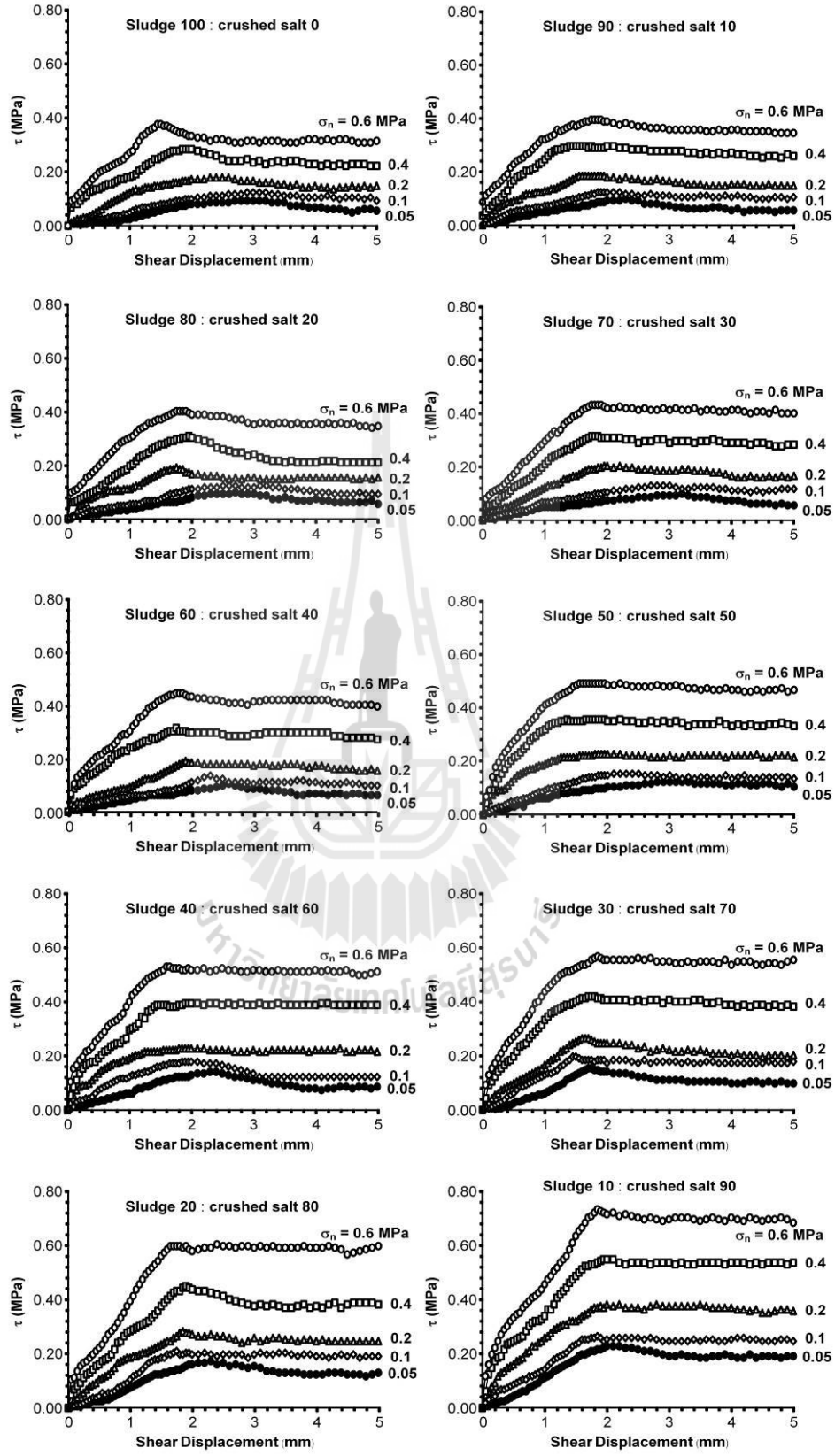

Figure 4.4 Shear stresses as a function of shear displacement.

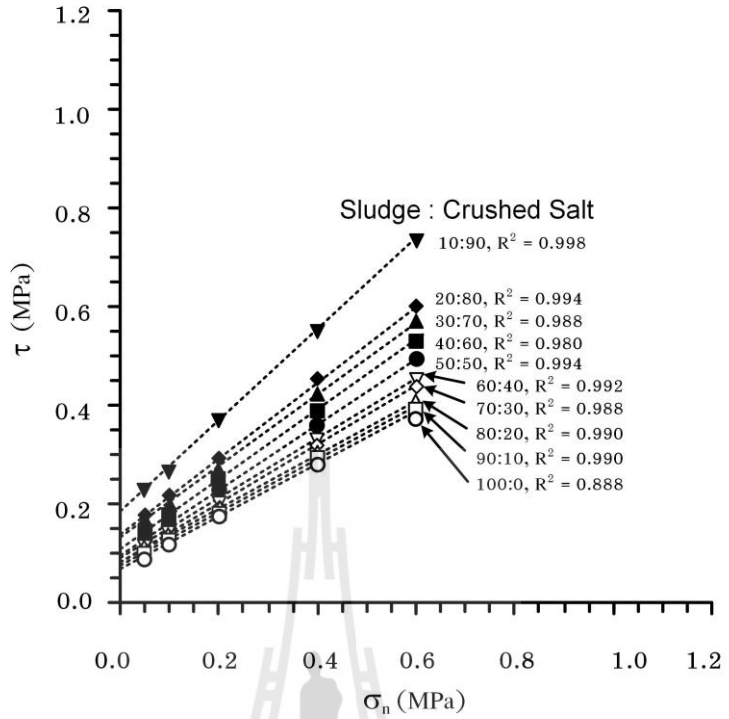

Figure 4.5 Shear strength as a function of normal stress.

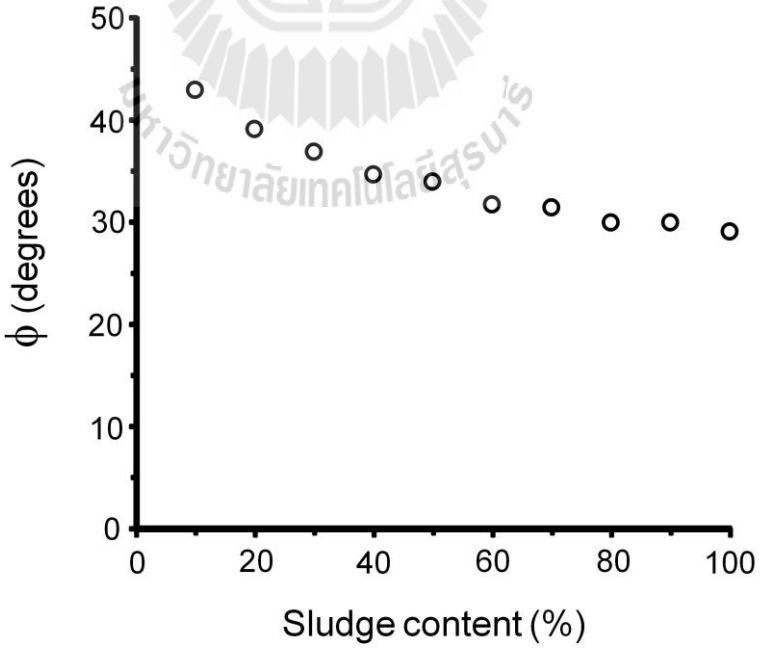

Figure 4.6 Friction angle as a function of sludge content.

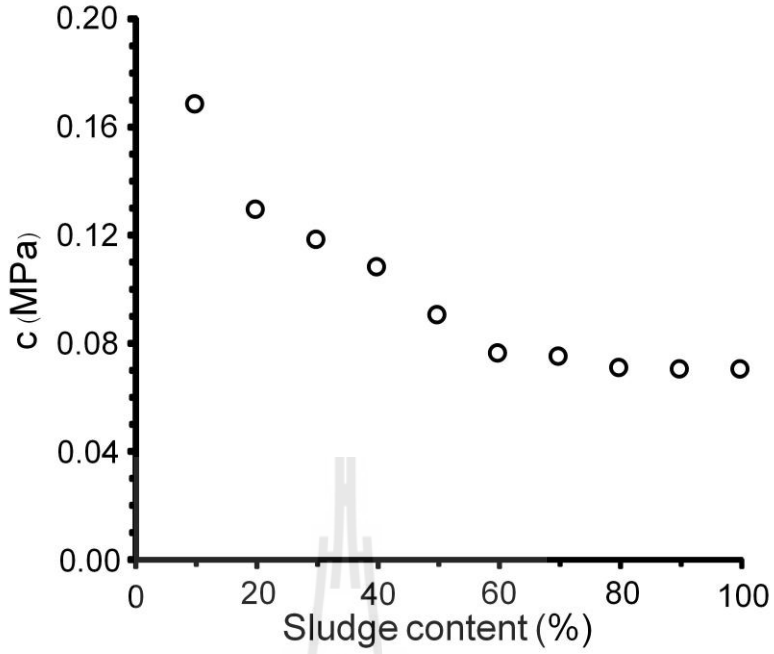

Figure 4.7 Cohesion as a function of sludge content.

Table 4.2 Direct shear test results.

S:C	c (kPa)	ϕ (degrees)	R^2
100:0	72	27	0.888
90:10	73	28	0.990
80:20	73	29	0.990
70:30	76	32	0.988
60:40	79	32	0.992
50:50	90	34	0.994
40:60	111	35	0.980
30:70	119	37	0.988
20:80	132	38	0.994
10:90	180	42	0.998

4.2.3 Permeability test

The flow testing is performed to determine intrinsic permeability of sludge-crushed salt mixtures by the constant head flow test. The compacted specimen are put into a PVC pipe. The internal diameter and height of the pipe is 98 mm and 178 mm, respectively. The test arrangement (Figure 4.6) comprises a PVC pipe, brine pump, needle valve used to maintain the constant head, and pipette (capacity 2 ml). The brine head is constant at 120 cm for all tests. The test is conducted by injecting brine into the PVC pipe that contains the mixture. The elapse time is recorded after brine flow through the compacted specimen to the pipette at every 1 ml. Each test condition is conducted at least 3 times to obtain the average result and to verify the repeatability of the results. The hydraulic conductivity (K) is property of material that a fluid can flow through pore spaces or fractures. It can be obtained by the equation:

$$K = VL/Aht \tag{4.7}$$

where V is collected volume of brine (m^3), L is length of mixture (15 cm), A is cross-section area of sample (0.0081 m^2), h is head difference of brine elevation and the sample (constant at 120 cm) and t is time period to collect V. The intrinsic permeability (k) is intrinsic property of the material structure. It can be determined from the equation:

$$k = K\mu/\gamma \tag{4.8}$$

where K is the coefficient of permeability (m/s), μ is dynamic viscosity of brine (0.001085 Pa·s) and γ is density of brine (11.772 kN/m^3).

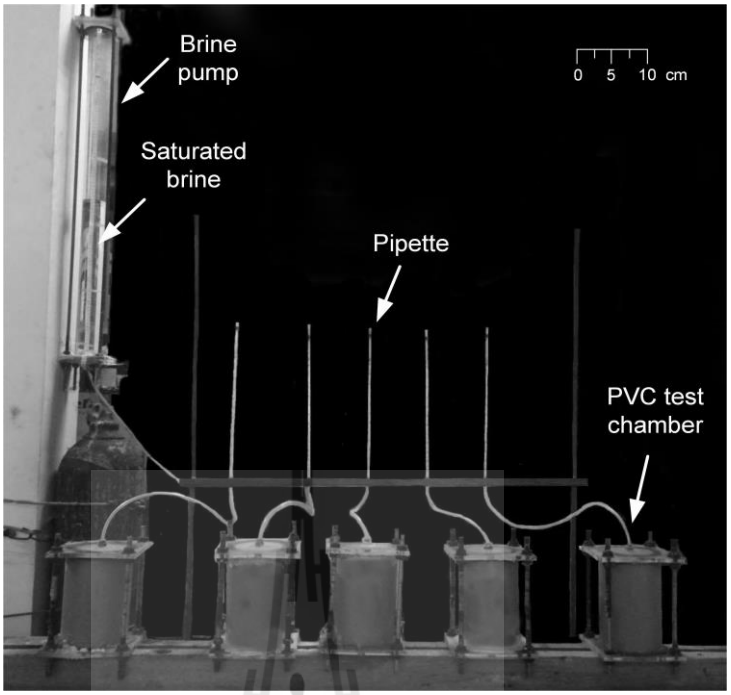

Figure 4.8 Flow test arrangement.

The results show that under saturated condition time has no effect on the hydraulic conductivity and intrinsic permeability of the samples (Figures 4.7 and 4.8). This may be because the test duration may not be enough for changing of mixture properties. The lowest limit of the measurement system is 10^{-17} m^2. Figures 4.9 and 4.10 indicate that the permeability of compacted mixtures decrease with increasing of sludge content. This is due to that the grain size of sludge is very small (<0.475 mm), and hence it can fill the void between crushed salt grains. It means the fluid can flow through the mixtures with lower velocity. The summary of results obtained from the constant head flow testing for 30 days are shown in Appendix A. The average permeability is shown in Table 4.3.

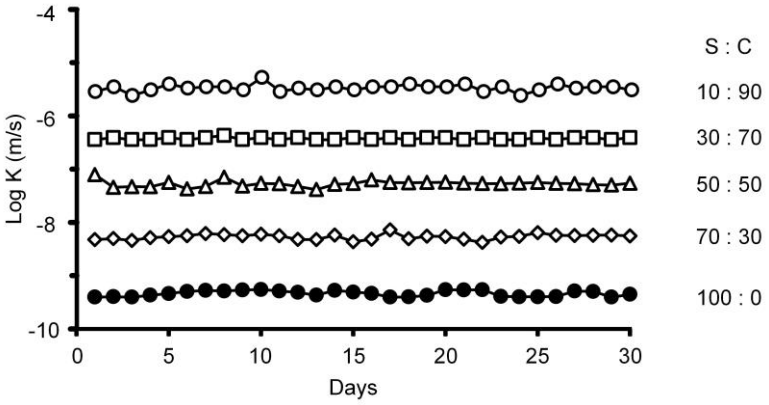

Figure 4.9 Hydraulic conductivity (K) as function of time.

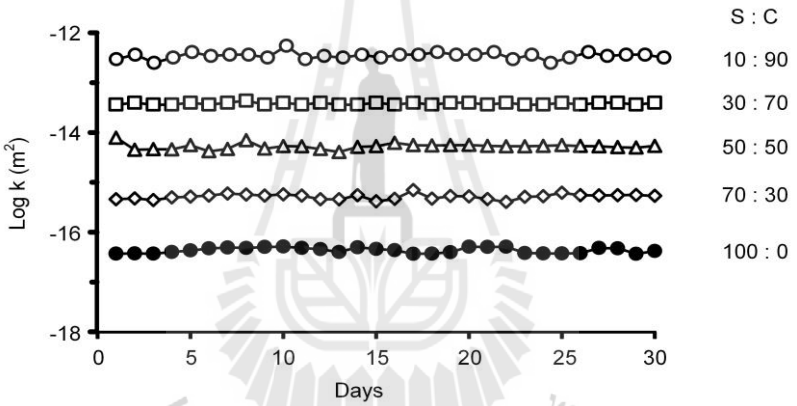

Figure 4.10 Intrinsic permeability (k) as function of time.

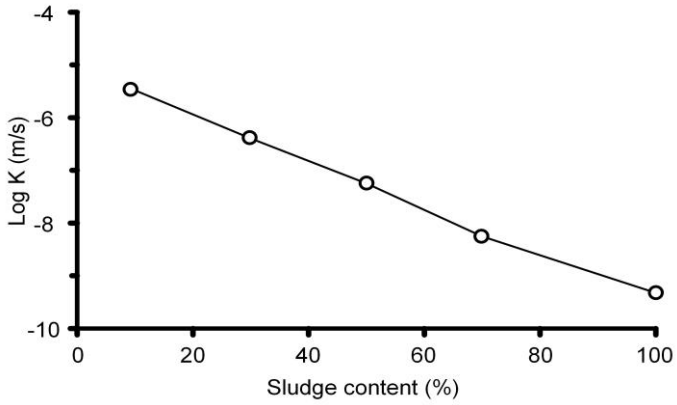

Figure 4.11 Hydraulic conductivity (K) as function of sludge content.

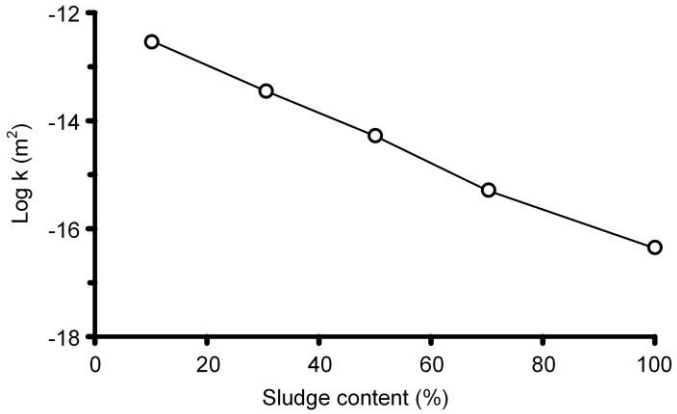

Figure 4.12 Intrinsic permeability (k) as function of sludge content.

Table 4.3 Average hydraulic properties from constant head permeability test results.

Sludge: crushed salt	**Flow rate, Q (m^3/s)**	**Hydraulic conductivity, K (m/s)**	**SD**	**Intrinsic permeability, k (m^2)**	**SD**
100:0	3.07×10^{-10}	4.73×10^{-10}	$\pm5.96\times10^{-11}$	4.36×10^{-17}	$\pm5.50\times10^{-18}$
70:30	3.63×10^{-9}	5.61×10^{-9}	$\pm6.67\times10^{-10}$	5.17×10^{-16}	$\pm6.15\times10^{-17}$
50:50	3.68×10^{-8}	5.68×10^{-8}	$\pm8.00\times10^{-9}$	5.23×10^{-15}	$\pm7.37\times10^{-16}$
30:70	2.62×10^{-7}	4.05×10^{-7}	$\pm2.07\times10^{-8}$	3.73×10^{-14}	$\pm1.91\times10^{-15}$
10:90	2.14×10^{-6}	3.30×10^{-6}	$\pm5.23\times10^{-7}$	3.04×10^{-13}	$\pm4.82\times10^{-14}$

CHAPTER V

COMPUTER SIMULATION

5.1 Introduction

The computer simulation (FLAC 4.0-Itasca, 1992) is used to determine the effectiveness of backfill in salt mines after the mine excavation completed. The effects of overburden thickness, room height and sludge contents on surface subsidence, and room and pillar deformation are investigated.

5.2 Input parameters

The stratigraphy of rock salt in Thailand has been compiled by many investigators (Japakasetr and Suwanish, 1977; Suwanich et al., 1982; Suwanich and Ratanajaruraks, 1986; Japakasetr, 1985). These data are obtained from the 194 exploration boreholes drilled in northeast of Thailand. In this study, the stratigraphic column of rock salt and clastic rock at Ban Hhao, Muang district, Udon Thani province (borehole no. K-089) is applied as an example for use in computer simulation (Figure 5.1). The properties of the materials are shown in Tables 5.1, to 5.3. The salt property parameters are obtained from the calibration by Samsri et al. (2010) and Sriapai et al. (2012). The clastic rock properties are taken from Crosby (2007) and the compacted material are obtained from this study. The simulated conditions vary the clastic rock thickness from 200, 250 to 300 m with the rock salt thickness of 30 m. The room height is varied from 6, 8 and 10 m.

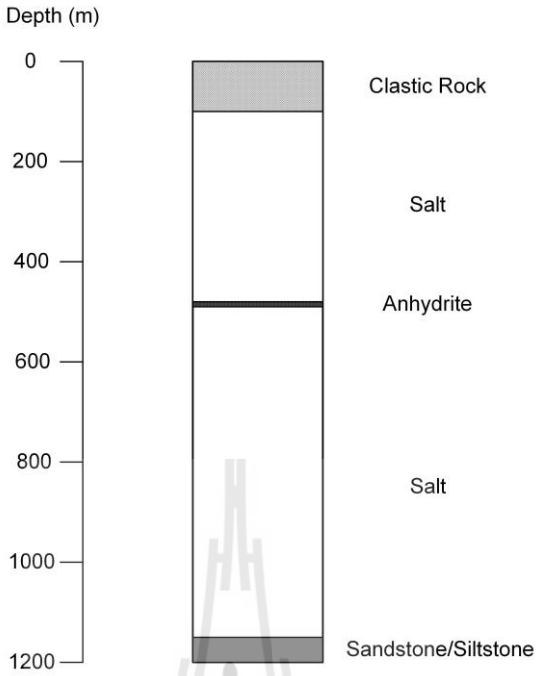

Figure 5.1 Stratigraphy of borehole no. K-089 at Ban Hhao, Muang district, Udon Thani province (Suwanich, 1986).

Table 5.1 Mechanical properties of clastic rock and rock salt for FLAC 4.0 simulations (Crosby 2007, Sriapai et al, 2012).

Parameters	Rock types	
	Clastic rock	Rock salt
Density, ρ (kg/m^3)	2,490	2,150
Bulk modulus, K (GPa)	1.70	2.22
Shear modulus, G (GPa)	0.30	1.67
Cohesion, c (MPa)	3.50	0.50
Internal friction angle, ϕ (Degrees)	25	50
Tension, T (MPa)	0.83	1.00

Table 5.2 Rock salt properties for FLAC 4.0 simulations (Samsri et al., 2010).

Parameters	Values
Elastic modulus, E_1 (GPa)	1.90
Spring constant in visco-elastic phase, E_2 (GPa)	5.79
Visco-plastic coefficient in steady-state phase, η1 (GPa.day)	0.34
Viscon-plastic coefficient in transient phase, η2 (GPa.day)	0.71
Density, γ (kg/m^3)	2,200

Table 5.3 Compacted material properties for FLAC 4.0 simulations.

Sludge-to-crushed salt ratios (S:C)	Properties				
	Density (kg/m^3)	Elastic modulus (GPa)	Poisson's ratios	Cohesion (kPa)	Friction angle (degrees)
20 : 80	2,010	2.50	0.130	132	38
40 : 60	1,950	2.35	0.105	111	35
60 : 40	1,910	2.10	0.087	79	32
80 : 20	1,810	1.70	0.08	73	29
100 : 0	1,660	1.60	0.07	72	27

The mesh density is designed to simulate the overburden layer, rock salt layer and underground opening. There are 500 to 700 elements covering the cross-section of the model. The duration before backfill is varied from 6, 12 to 24 months, overburden thickness is varied from 200, 250 and 300 m, and opening height is varied from 6, 8 and 10 m.

5.3 Simulation results

The computer simulations are calculated up to 50 years after backfill process. The surface subsidence, and roof, floor and pillar deformations under various overburden thickness and room heights are evaluated.

5.3.1 Duration before backfill

The effects of duration before backfill on underground mine stability are studied here. The boundary conditions are shown in Figure 5.2. The input parameters include the overburden thickness = 200 m, room height = 6 m and salt thickness = 30 m. The sludge-to-crushed salt (S:C) ratios are 100:0, 80:20, 60:40, 40:60 and 20:80. The results indicate that the duration before backfill has small effect on subsidence and opening deformation. The results are shown in Tables 5.4 through 5.8.

5.3.2 Opening height

The effect of opening height is investigated by varying the opening heights from 6, 8 to 10 m, where the overburden thickness is constant at 300 m, the salt thickness is 30 m and duration before backfill is 24 months. The mesh is shown in Figure 5.8. The surface subsidence, roof, floor and pillar deformations after 50 years with backfill and without backfill conditions are observed. The results are shown in Tables 5.9 through 5.13.

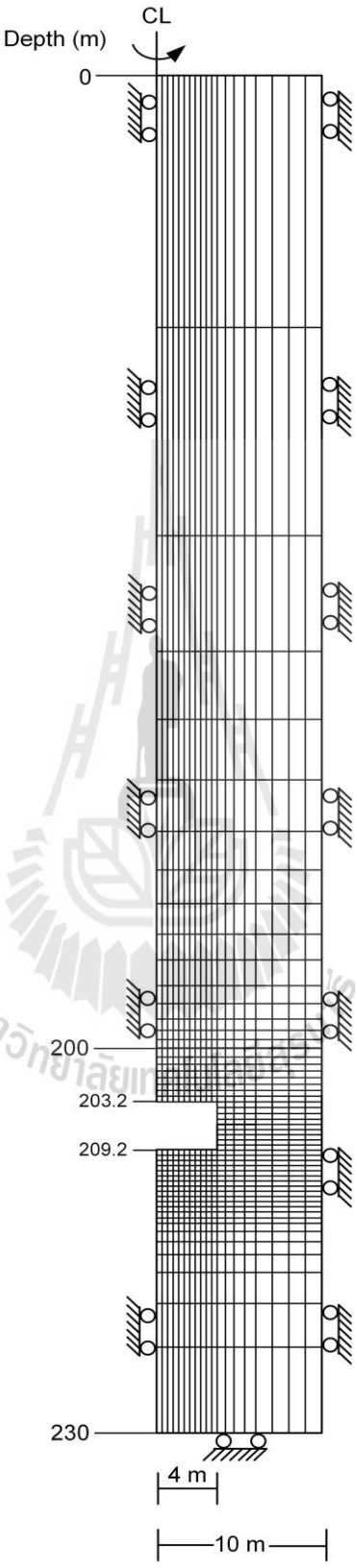

Figure 5.2 Mesh boundary conditions used in this study.

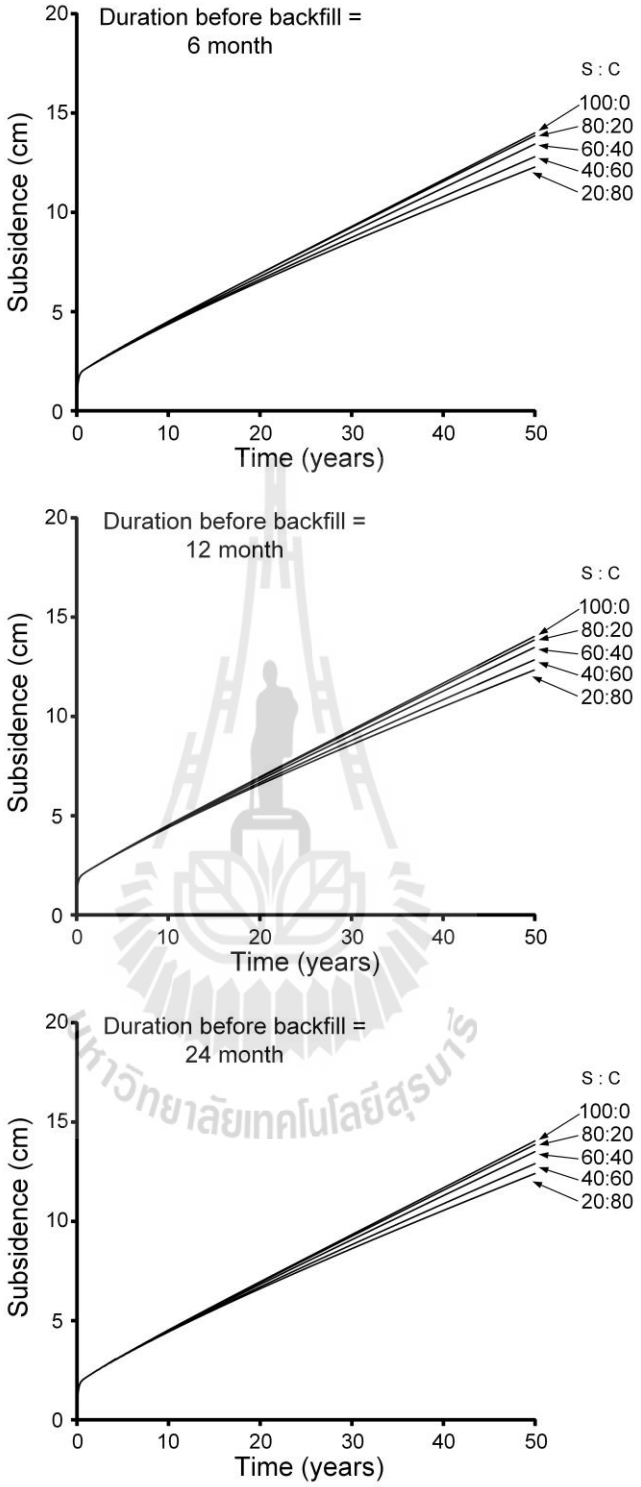

Figure 5.3 Surface subsidence as a function of time with different S:C ratios where overburden thicknesses = 200 m, duration before backfill = 6, 12 and 24 months, and opening height = 6 m.

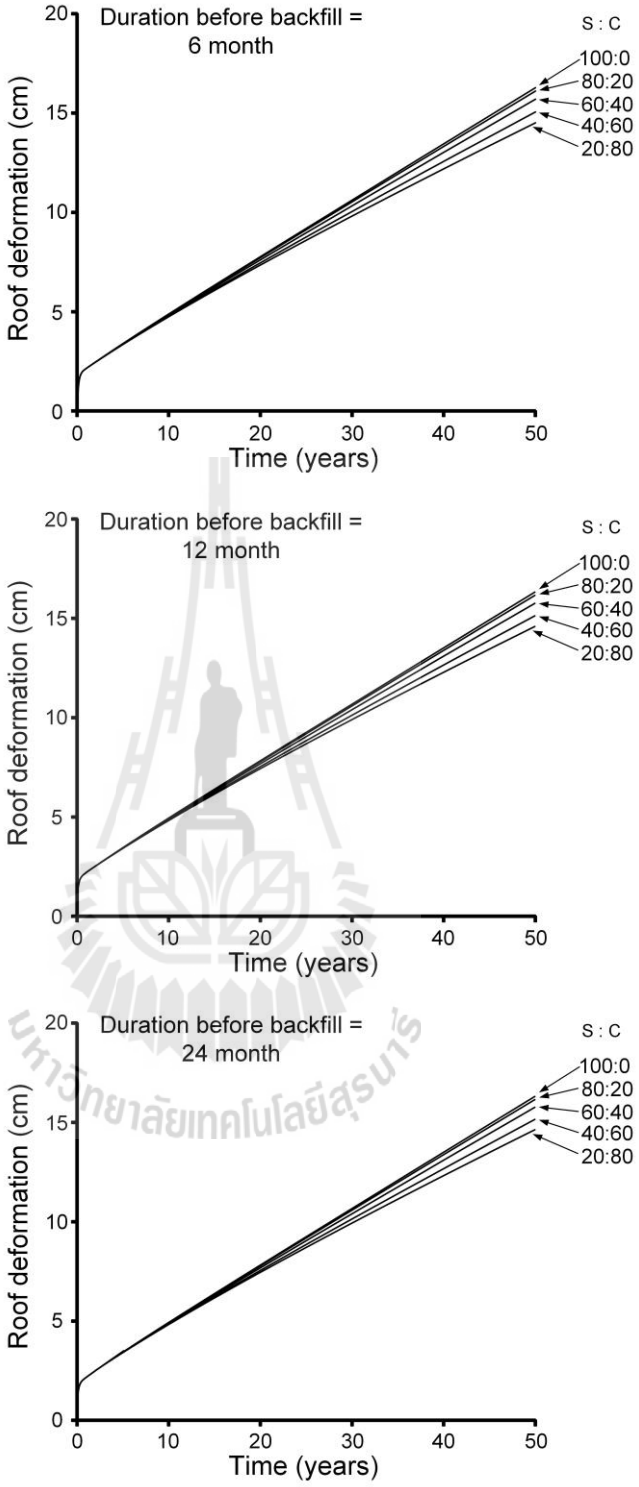

Figure 5.4 Roof deformation as a function of time with different S:C ratios where overburden thicknesses = 200 m, duration before backfill = 6, 12 and 24 months, and opening height = 6 m.

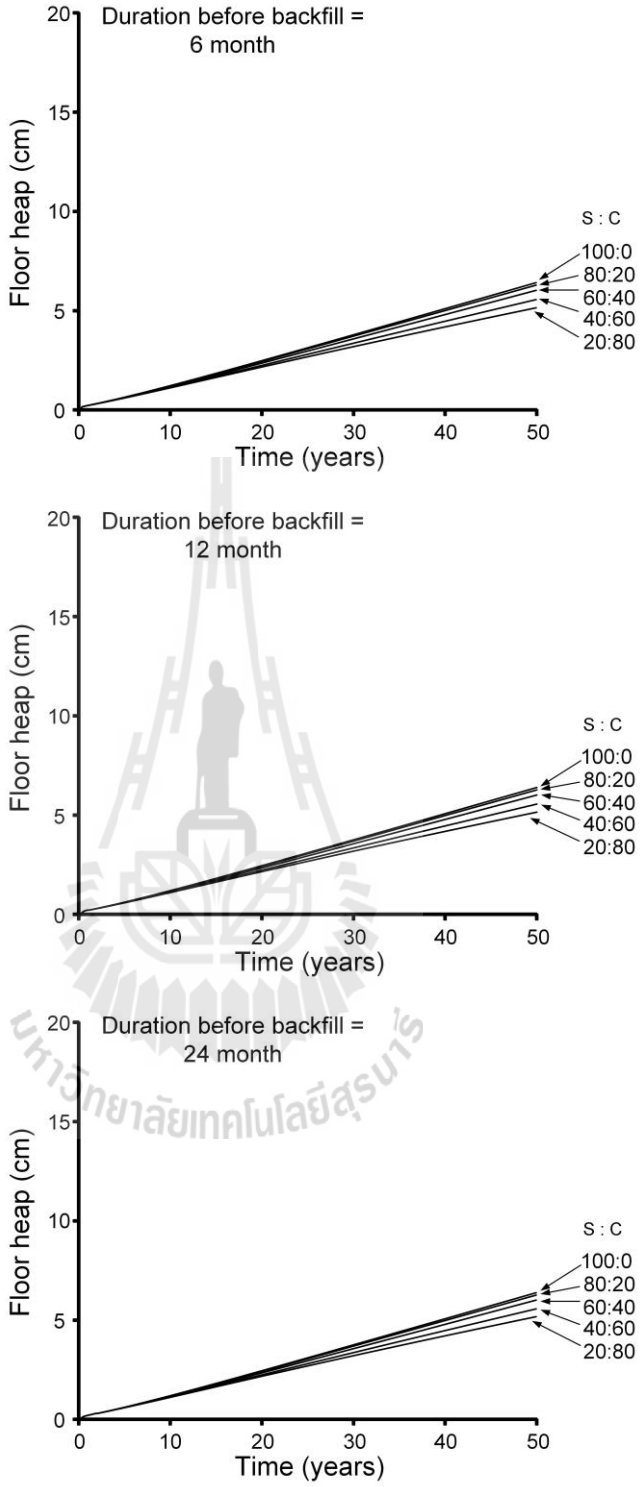

Figure 5.5 Floor heap as a function of time with different S:C ratios where overburden thicknesses = 200 m, duration before backfill = 6, 12 and 24 months, and opening height = 6 m.

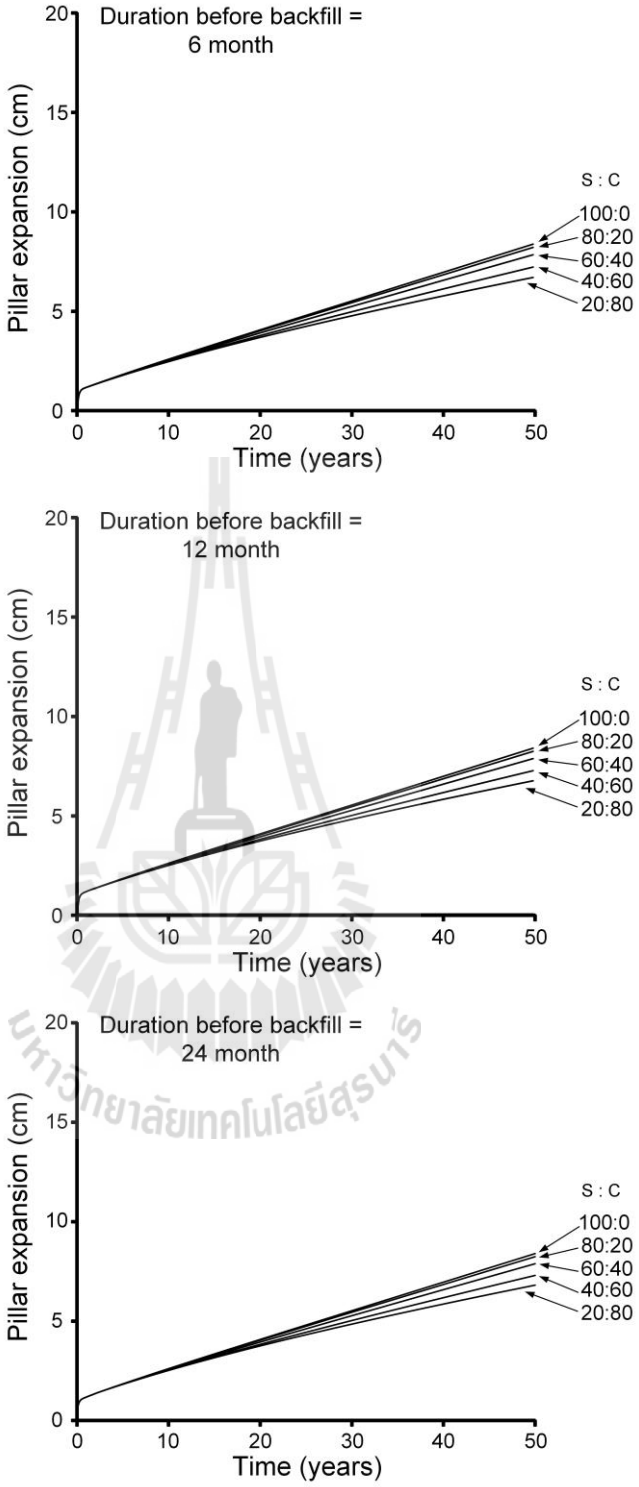

Figure 5.6 Pillar expansion as a function of time with different S:C ratios where overburden thicknesses = 200 m, duration before backfill = 6, 12 and 24 months, and opening height = 6 m.

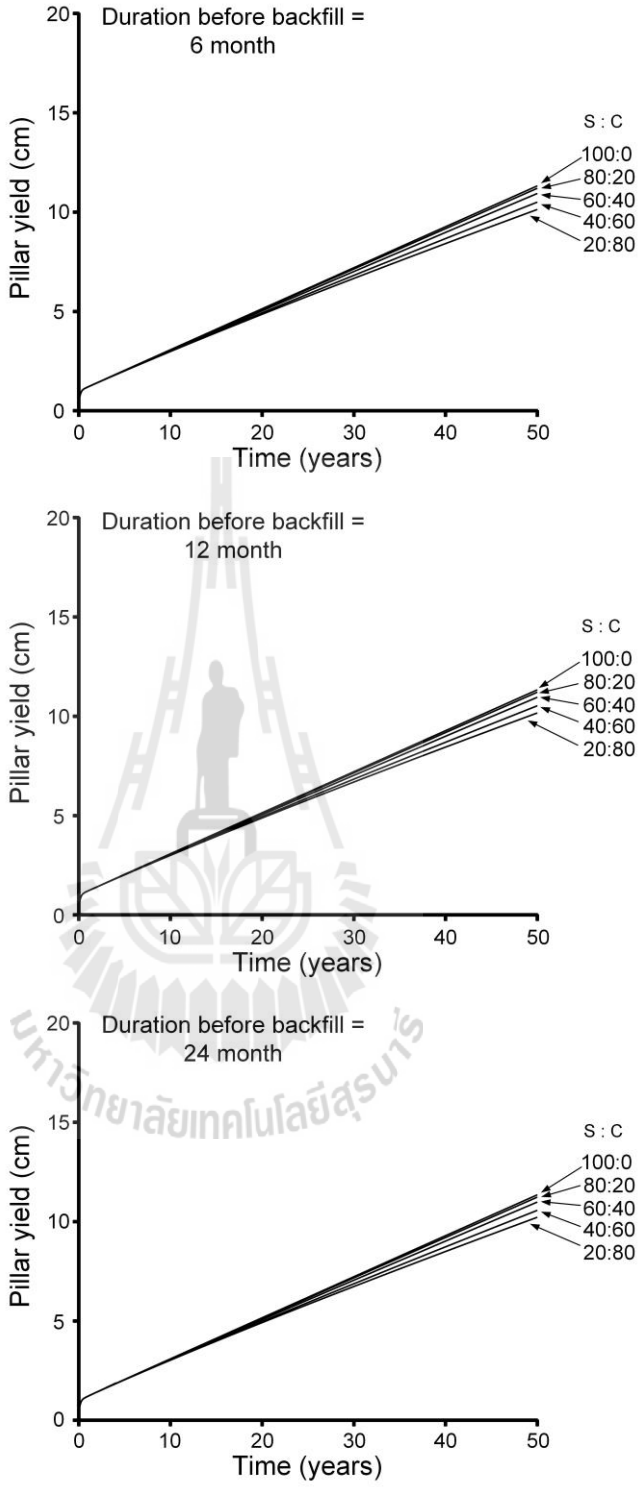

Figure 5.7 Pillar yield as a function of time with different S:C ratios where overburden thicknesses = 200 m, duration before backfill = 6, 12 and 24 months, and opening height = 6 m.

Table 5.4 Results of surface subsidence.

Input parameters			Surface subsidence after 50 years (cm)					
Thickness overburden (m)	Duration before backfill (Months)	Opening height (m)	No fill	S:C = 100:0	S:C = 80:20	S:C = 60:40	S:C = 40:60	S:C = 20:80
200	6	6	14.91	14.00	13.86	13.44	12.80	12.28
200	12	6	14.91	14.02	13.84	13.46	12.84	12.33
200	24	6	14.91	14.04	13.86	13.50	12.90	12.40

Table 5.5 Results of roof deformation.

Input parameters			Roof deformation after 50 years (cm)					
Thickness overburden (m)	Duration before backfill (Months)	Opening height (m)	No fill	S:C = 100:0	S:C = 80:20	S:C = 60:40	S:C = 40:60	S:C = 20:80
200	6	6	17.26	16.29	16.13	15.73	15.10	14.56
200	12	6	17.26	16.29	16.13	15.73	15.10	14.56
200	24	6	17.26	16.31	16.15	15.77	15.16	14.64

Table 5.6 Results of floor heap.

Input parameters			Floor heap after 50 years (cm)					
Thickness overburden (m)	Duration before backfill (Months)	Opening height (m)	No fill	S:C = 100:0	S:C = 80:20	S:C = 60:40	S:C = 40:60	S:C = 20:80
200	6	6	6.99	6.39	6.27	6.00	5.54	5.12
200	12	6	6.99	6.40	6.28	6.02	5.56	5.15
200	24	6	6.99	6.41	6.29	6.64	5.60	5.20

Table 5.7 Results of pillar expansion.

Input parameters			Pillar expansion after 50 years (cm)					
Thickness overburden (m)	Duration before backfill (Months)	Opening height (m)	No fill	S:C = 100:0	S:C = 80:20	S:C = 60:40	S:C = 40:60	S:C = 20:80
200	6	6	9.20	8.37	8.21	7.84	7.22	6.69
200	12	6	9.20	8.38	8.22	7.86	7.25	6.74
200	24	6	9.20	8.40	8.24	7.89	7.30	6.81

Table 5.8 Results of pillar yield.

Input parameters			Pillar yield after 50 years (cm)					
Thickness overburden (m)	Duration before backfill (Months)	Opening height (m)	No fill	S:C = 100:0	S:C = 80:20	S:C = 60:40	S:C = 40:60	S:C = 20:80
200	6	6	12.00	11.31	11.19	10.93	10.50	10.13
200	12	6	12.00	11.32	11.21	10.95	10.52	10.16
200	24	6	12.00	11.34	11.22	10.98	10.56	10.21

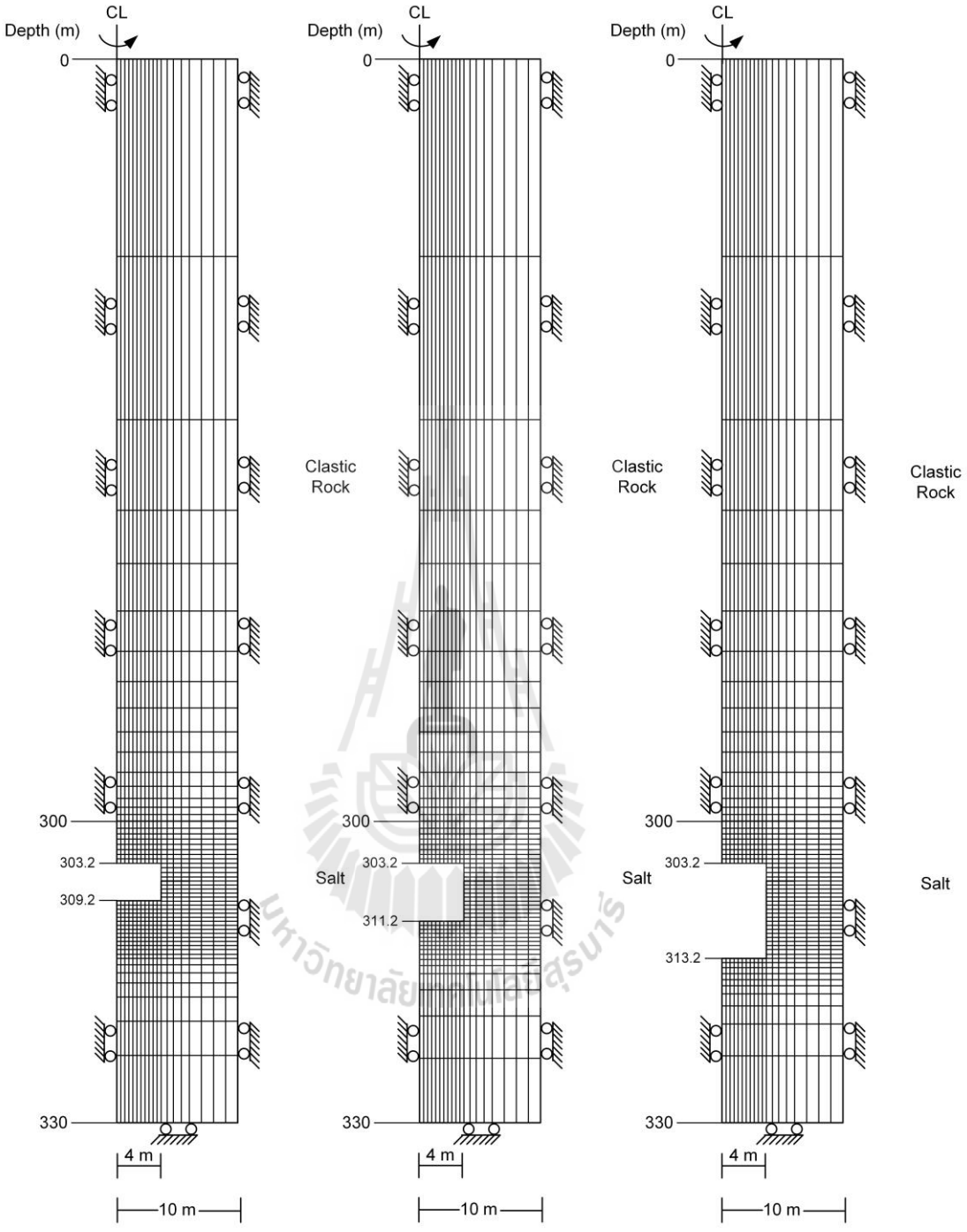

Figure 5.8 Finite difference mesh for overburden thickness = 300 m, rock salt = 30 m and opening height = 6, 8 and 10 m.

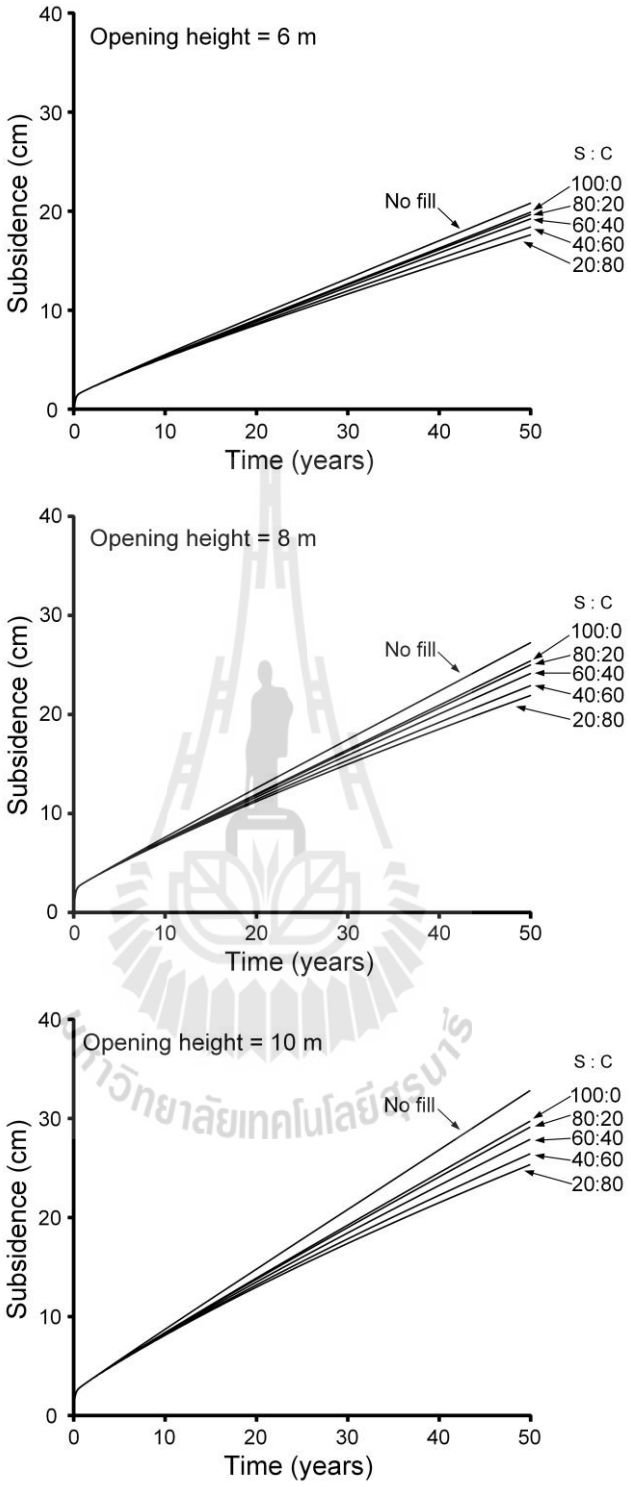

Figure 5.9 Surface subsidence as a function of time for different S:C ratios where overburden thicknesses = 300 m, duration before backfill = 24 months and opening height = 6, 8 and 10 m**.**

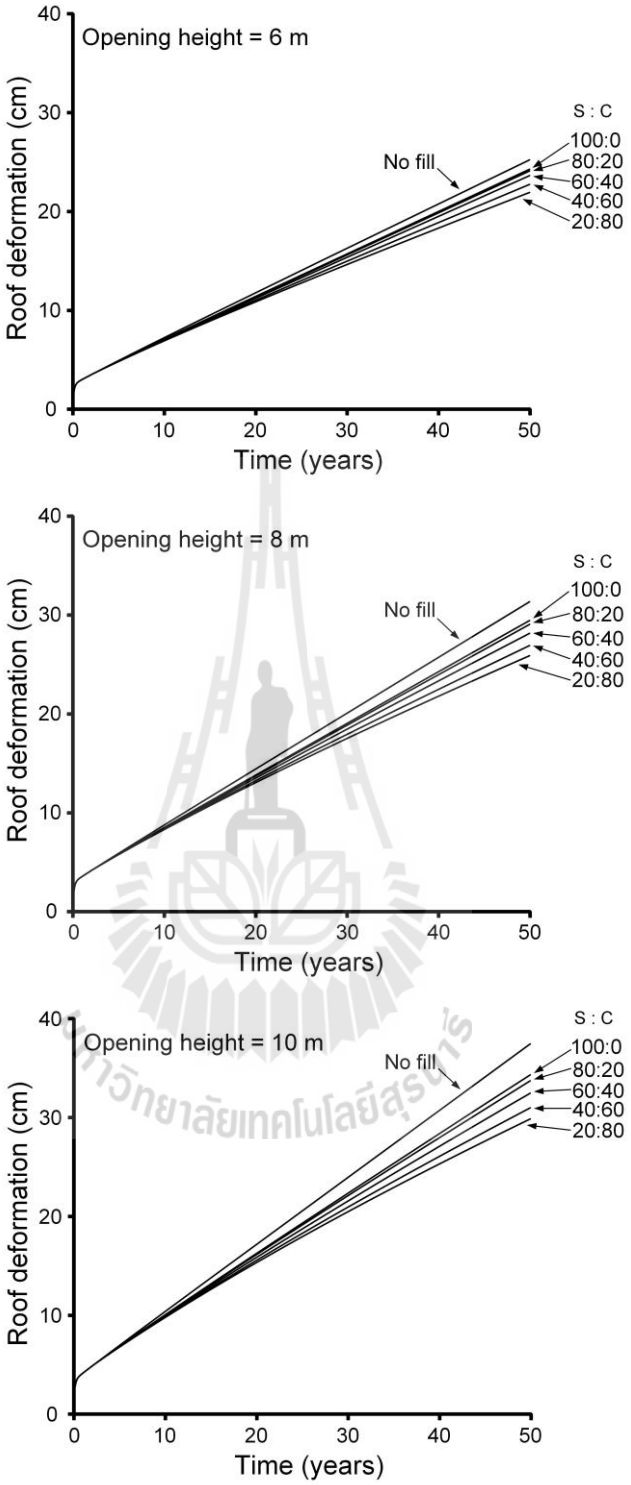

Figure 5.10 Roof deformation as a function of time for different S:C ratios where overburden thicknesses = 300 m, duration before backfill = 24 months and opening height = 6, 8 and 10 m**.**

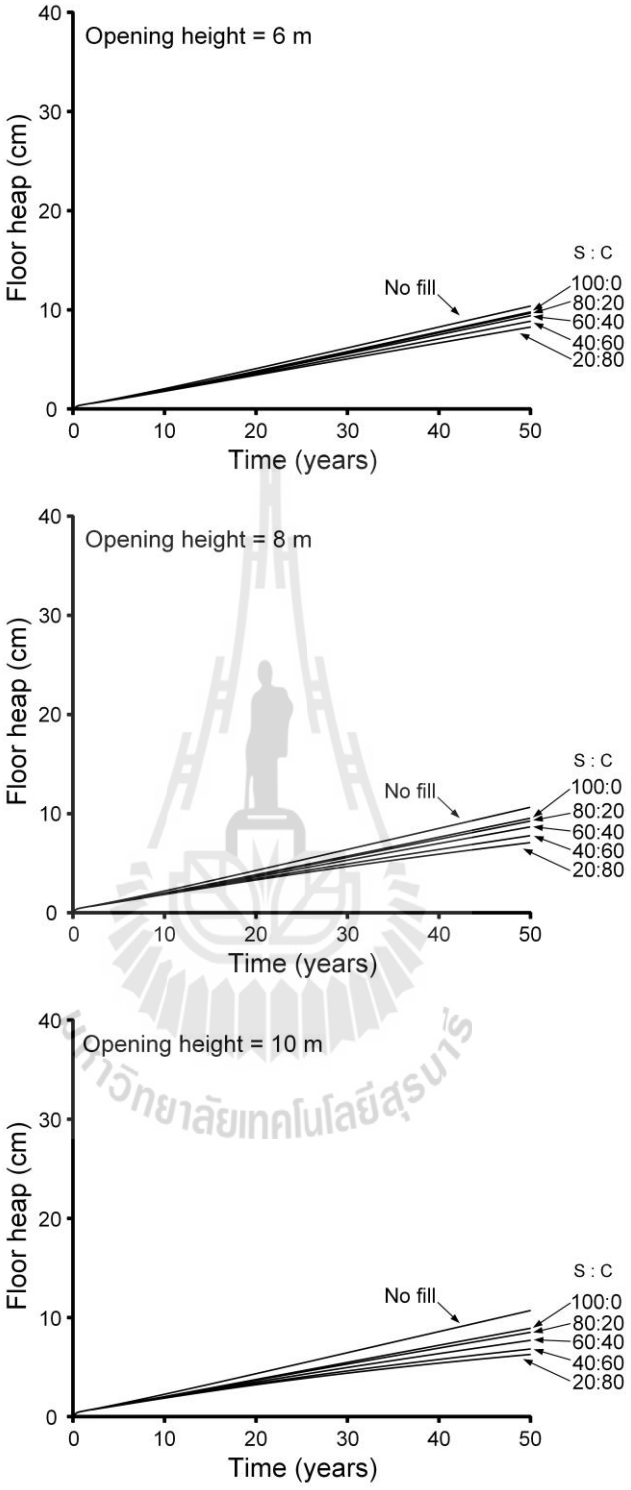

Figure 5.11 Floor heap as a function of time for different S:C ratios where overburden thicknesses = 300 m, duration before backfill = 24 months and opening height = 6, 8 and 10 m.

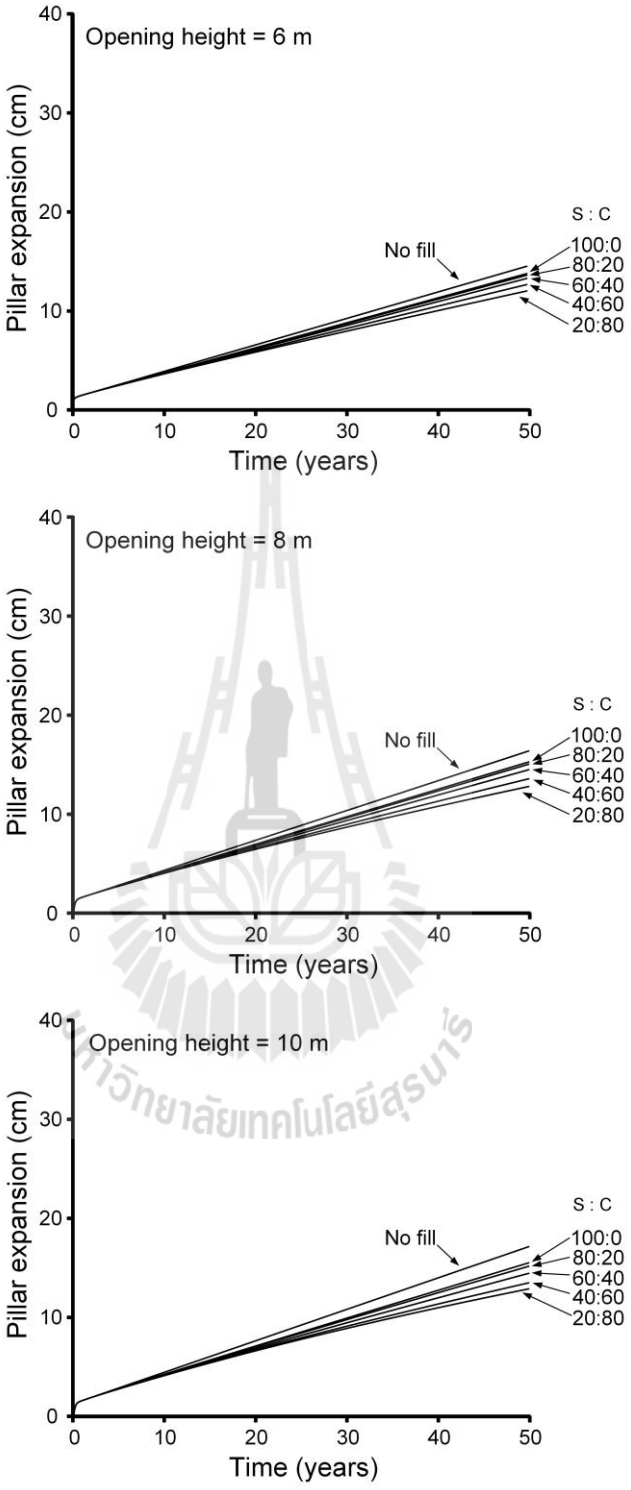

Figure 5.12 Pillar expansion as a function of time for different S:C ratios where overburden thicknesses = 300 m, duration before backfill = 24 months and opening height = 6, 8 and 10 m.

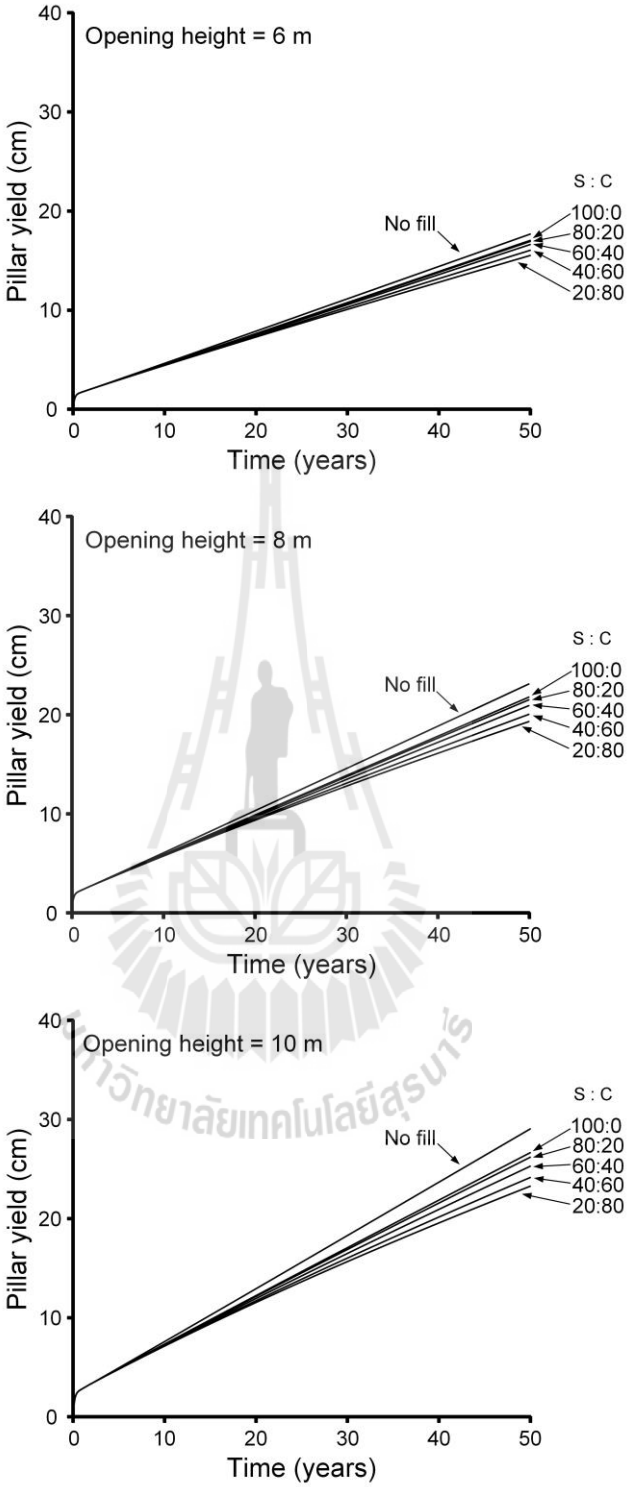

Figure 5.13 Pillar yield as a function of time for different S:C ratios where overburden thicknesses = 300 m, duration before backfill = 24 months and opening height = 6, 8 and 10 m.

Table 5.9 Results of surface subsidence.

Input parameters			Surface subsidence after 50 years (cm)					
Thickness overburden (m)	Duration before backfill (Months)	Opening height (m)	No fill	S:C = 100:0	S:C = 80:20	S:C = 60:40	S:C = 40:60	S:C = 20:80
300	24	6	20.80	19.89	19.65	19.22	18.40	17.61
300	24	8	27.23	25.39	24.99	24.12	22.89	21.90
300	24	10	32.81	29.72	29.12	27.88	26.42	25.33

Table 5.10 Results of roof deformation.

Input parameters			Roof deformation after 50 years (cm)					
Thickness overburden (m)	Duration before backfill (Months)	Opening height (m)	No fill	S:C = 100:0	S:C = 80:20	S:C = 60:40	S:C = 40:60	S:C = 20:80
300	24	6	25.26	24.31	24.14	23.67	22.78	21.96
300	24	8	31.32	29.42	29.03	28.13	26.89	25.86
300	24	10	37.42	34.28	33.69	32.43	30.95	29.83

Table 5.11 Results of floor heap.

Input parameters			Floor heap after 50 years (cm)					
Thickness overburden (m)	Duration before backfill (Months)	Opening height (m)	No fill	S:C = 100:0	S:C = 80:20	S:C = 60:40	S:C = 40:60	S:C = 20:80
300	24	6	10.34	9.75	9.63	9.37	8.81	8.23
300	24	8	10.60	9.49	9.21	8.63	7.74	7.04
300	24	10	10.72	8.93	8.52	7.71	6.84	6.29

Table 5.12 Results of pillar expansion.

Input parameters			Pillar expansion after 50 years (cm)					
Thickness overburden (m)	Duration before backfill (Months)	Opening height (m)	No fill	S:C = 100:0	S:C = 80:20	S:C = 60:40	S:C = 40:60	S:C = 20:80
300	24	6	14.53	13.78	13.62	13.30	12.68	12.63
300	24	8	16.31	15.20	14.98	14.42	13.51	12.73
300	24	10	17.17	15.55	15.20	14.49	13.53	12.92

Table 5.13 Results of pillar yield.

Input parameters			Pillar yield after 50 years (cm)					
Thickness overburden (m)	Duration before backfill (Months)	Opening height (m)	No fill	S:C = 100:0	S:C = 80:20	S:C = 60:40	S:C = 40:60	S:C = 20:80
300	24	6	17.65	17.01	16.90	16.59	16.01	15.49
300	24	8	23.07	21.74	21.47	20.89	20.01	19.28
300	24	10	29.05	26.66	26.19	25.29	24.15	23.27

5.3.3 Overburden thicknesses

The effect of overburden thickness is studied by varying the thickness from 200, 250 to 300 m., where the salt thickness is 30 m, opening height is 4 m and duration before backfill is 24 months. The boundary conditions are shown in Figure 5.14. The deformations after 50 years with backfill and without backfill conditions are shows in Tables 14 through 18.

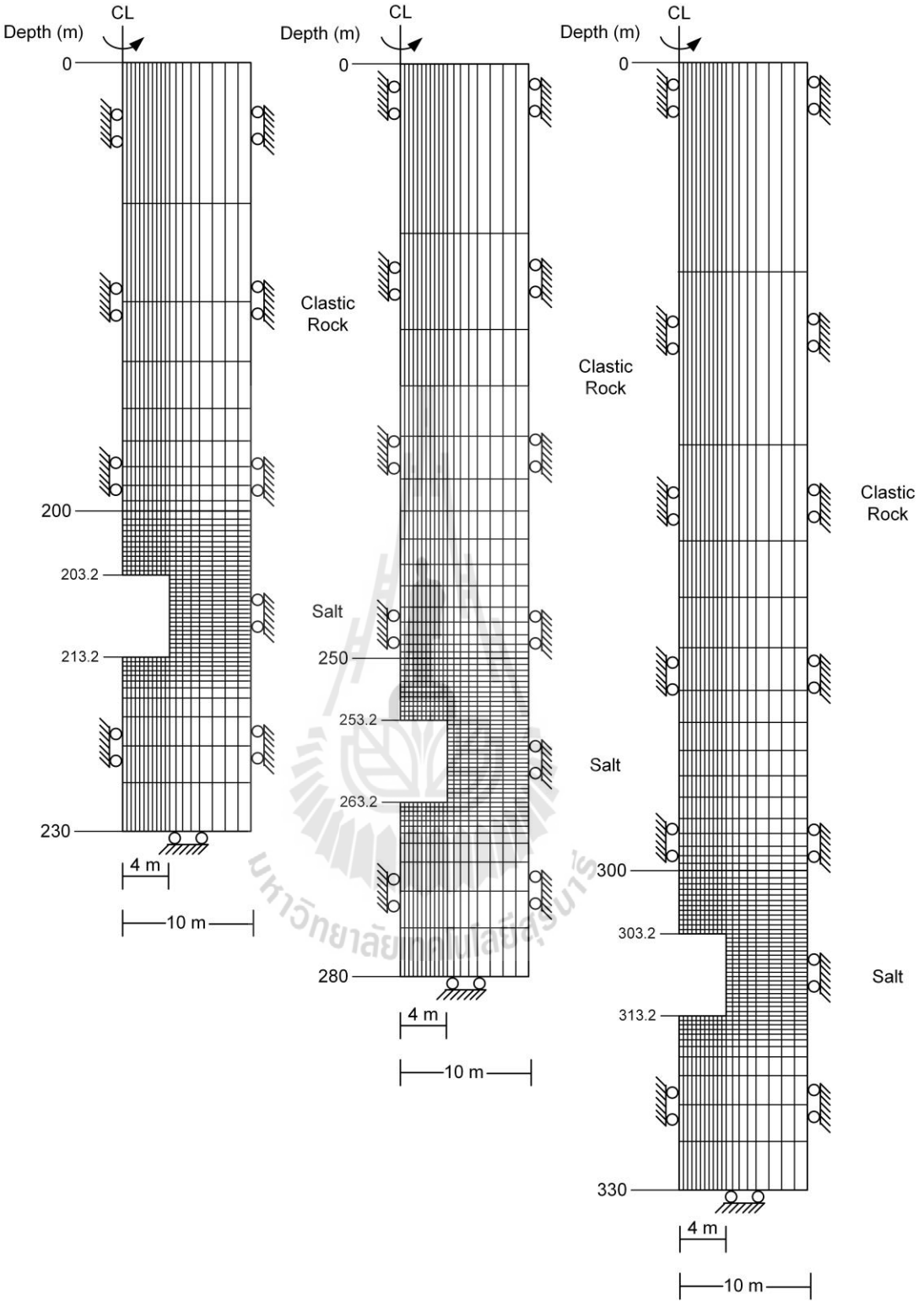

Figure 5.14 Finite difference mesh for overburden thickness = 200, 250 and 300 m, rock salt = 30 m and opening height = 10 m.

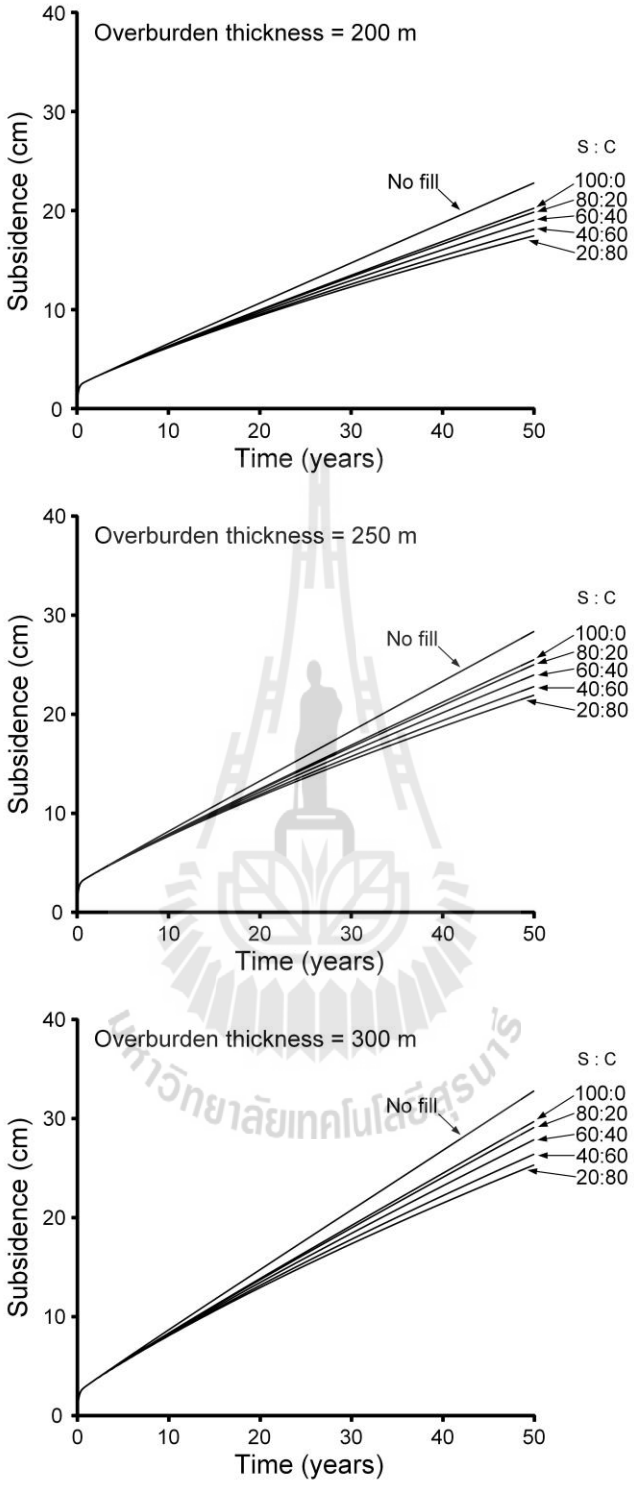

Figure 5.15 Surface subsidence as a function of time for different S:C ratios where overburden thicknesses = 200, 250 and 300 m, duration before backfill = 24 months and opening height = 10 m.

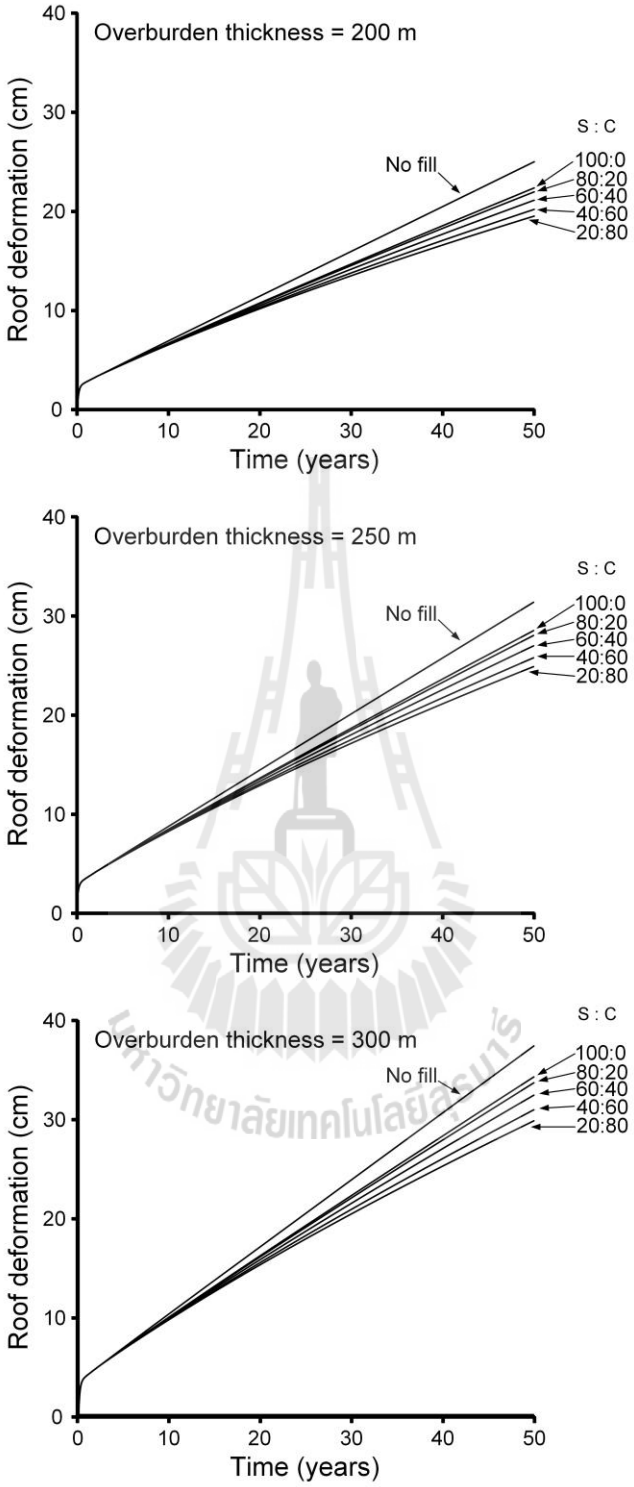

Figure 5.16 Roof deformation as a function of time for different S:C ratios where overburden thicknesses = 200, 250 and 300 m, duration before backfill = 24 months and opening height = 10 m.

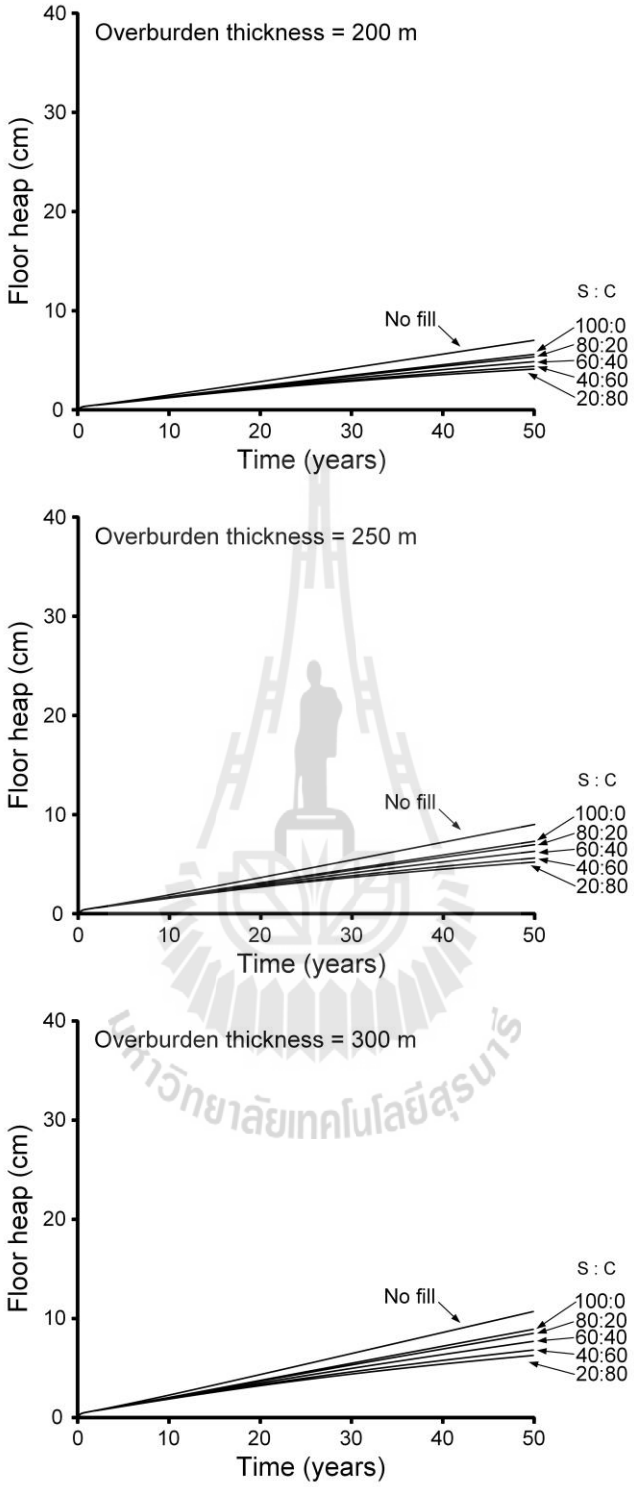

Figure 5.17 Floor heap as a function of time for different S:C ratios where overburden thicknesses = 200, 250 and 300 m, duration before backfill = 24 months and opening height = 10 m.

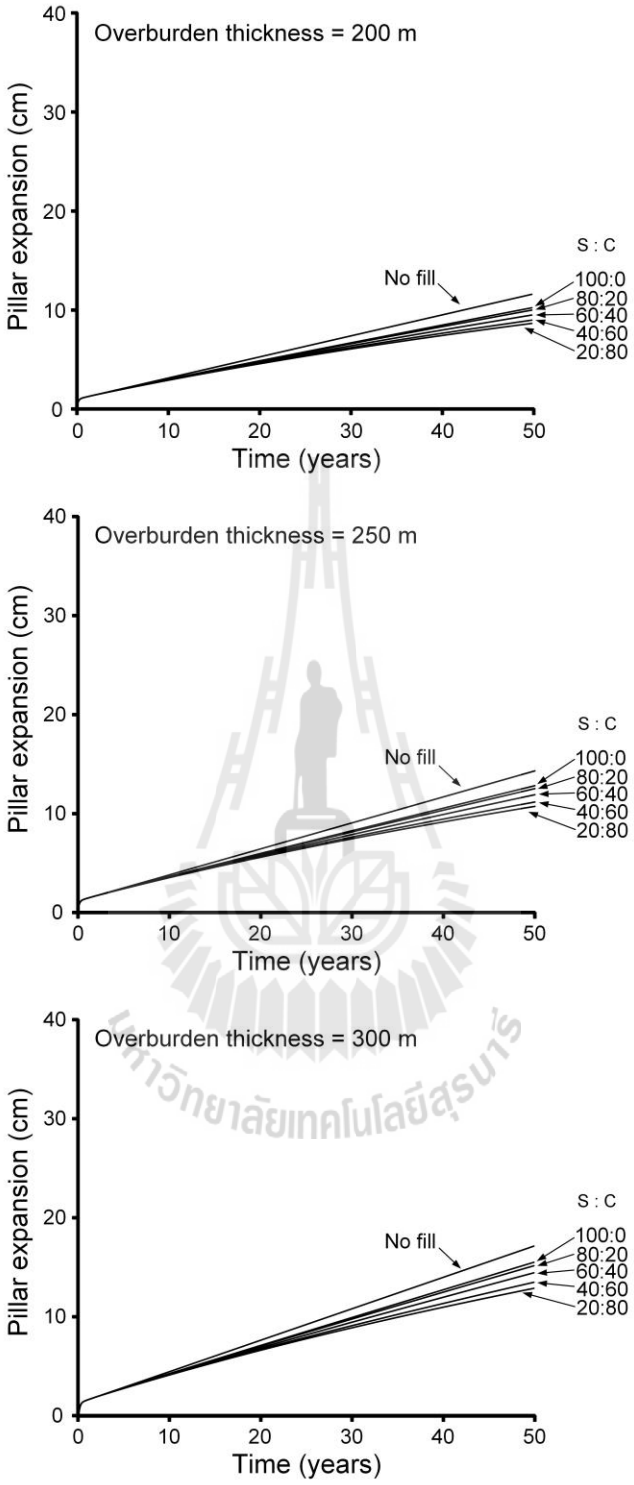

Figure 5.18 Pillar expansion as a function of time for different S:C ratios where overburden thicknesses = 200, 250 and 300 m, duration before backfill = 24 months and opening height = 10 m.

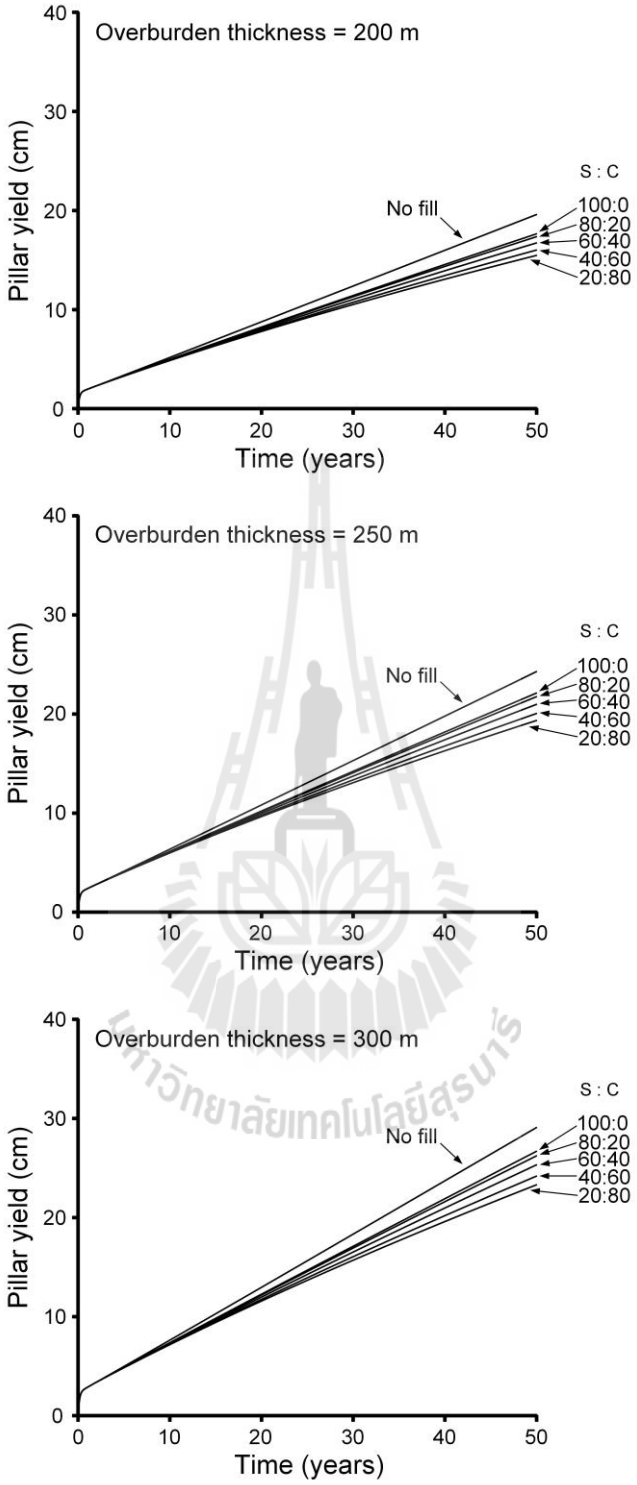

Figure 5.19 Pillar yield as a function of time for different S:C ratios where overburden thicknesses = 200, 250 and 300 m, duration before backfill = 24 months and opening height = 10 m.

Table 5.14 Results of surface subsidence.

Input parameters			Surface subsidence after 50 years (cm)					
Thickness overburden (m)	Duration before backfill (Months)	Opening height (m)	No fill	S:C = 100:0	S:C = 80:20	S:C = 60:40	S:C = 40:60	S:C = 20:80
200	24	10	22.78	20.23	19.84	19.01	18.11	17.45
250	24	10	28.32	25.47	24.97	23.93	22.76	21.89
300	24	10	32.81	29.72	29.12	27.88	26.42	25.33

Table 5.15 Results of roof deformation.

Input parameters			Roof deformation after 50 years (cm)					
Thickness overburden (m)	Duration before backfill (Months)	Opening height (m)	No fill	S:C = 100:0	S:C = 80:20	S:C = 60:40	S:C = 40:60	S:C = 20:80
200	24	10	24.99	22.34	21.95	21.11	20.18	19.50
250	24	10	31.36	28.50	28.01	26.96	25.76	24.86
300	24	10	37.42	34.28	33.69	32.43	30.95	29.83

Table 5.16 Results of floor heap.

Input parameters			Floor heap after 50 years (cm)					
Thickness overburden (m)	Duration before backfill (Months)	Opening height (m)	No fill	S:C = 100:0	S:C = 80:20	S:C = 60:40	S:C = 40:60	S:C = 20:80
200	24	10	6.98	5.57	5.32	4.83	4.36	4.08
250	24	10	8.98	7.28	6.94	6.27	5.59	5.18
300	24	10	10.72	8.93	8.52	7.71	6.84	6.29

Table 5.17 Results of pillar expansion.

Input parameters			Pillar expansion after 50 years (cm)					
Thickness overburden (m)	Duration before backfill (Months)	Opening height (m)	No fill	S:C = 100:0	S:C = 80:20	S:C = 60:40	S:C = 40:60	S:C = 20:80
200	24	10	11.48	10.13	9.89	9.39	8.88	8.55
250	24	10	14.33	12.83	12.83	11.91	11.18	10.73
300	24	10	17.17	15.55	15.20	14.49	13.53	12.92

Table 5.18 Results of pillar yield.

Input parameters			Pillar yield after 50 years (cm)					
Thickness overburden (m)	Duration before backfill (Months)	Opening height (m)	No fill	S:C = 100:0	S:C = 80:20	S:C = 60:40	S:C = 40:60	S:C = 20:80
200	24	10	19.56	17.61	17.33	16.70	15.98	15.44
250	24	10	24.32	22.15	21.78	21.01	20.08	19.38
300	24	10	29.05	26.66	26.19	25.29	24.15	23.27

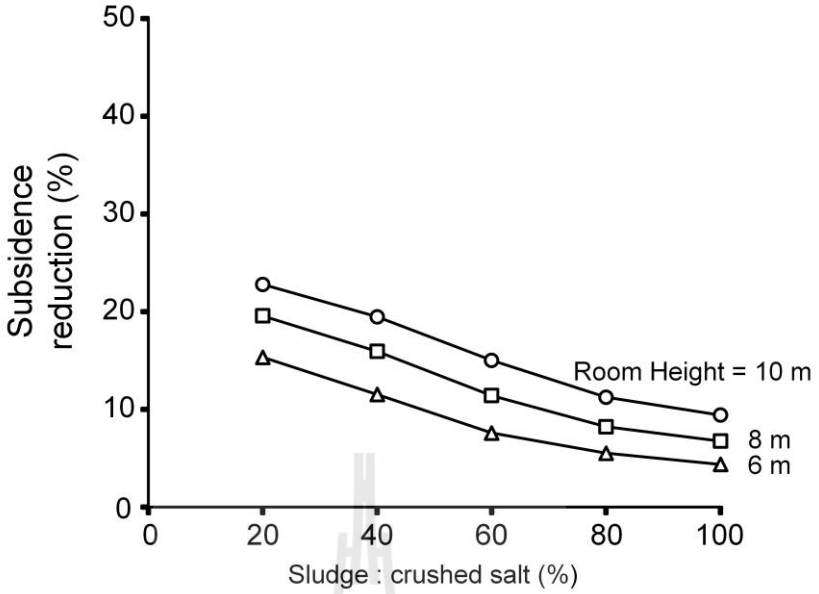

Figure 5.20 Subsidence reduction as a function of sludge content.

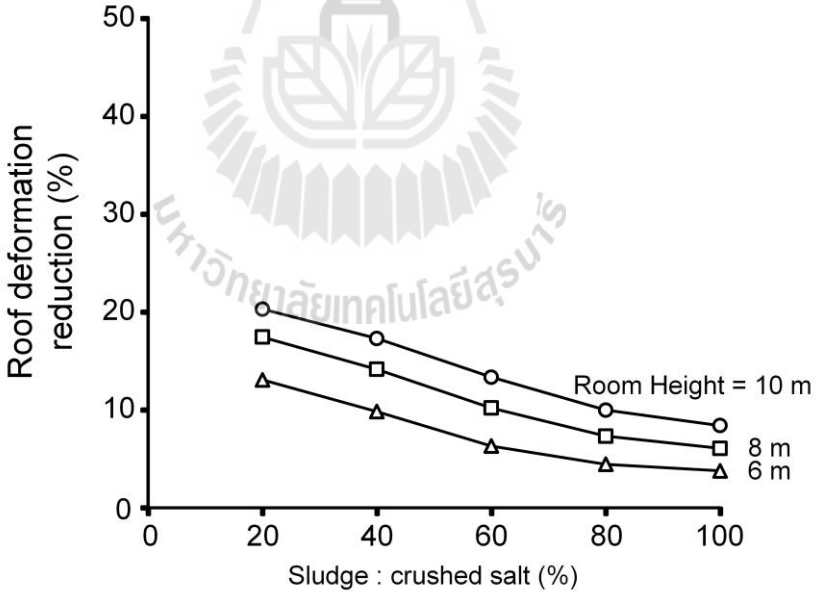

Figure 5.21 Roof deformation reduction as a function of sludge content.

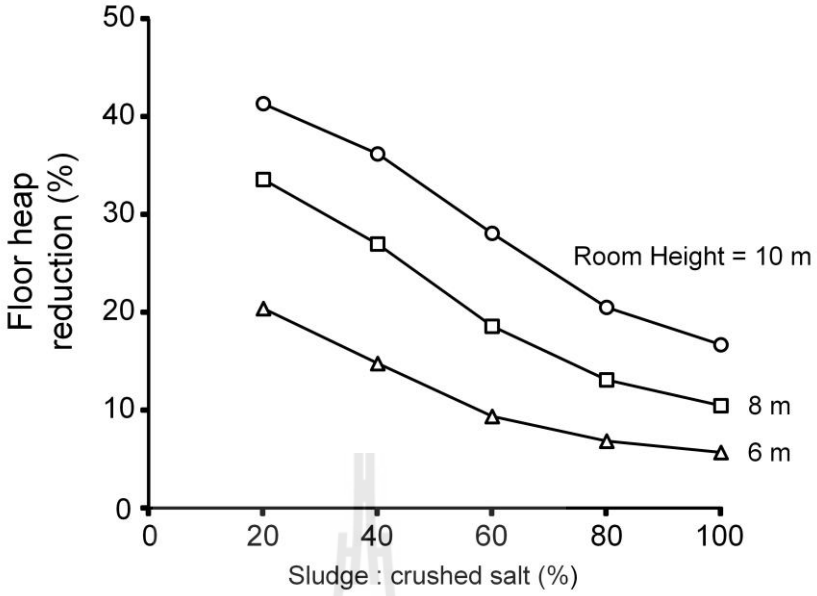

Figure 5.22 Floor heap reduction as a function of sludge content.

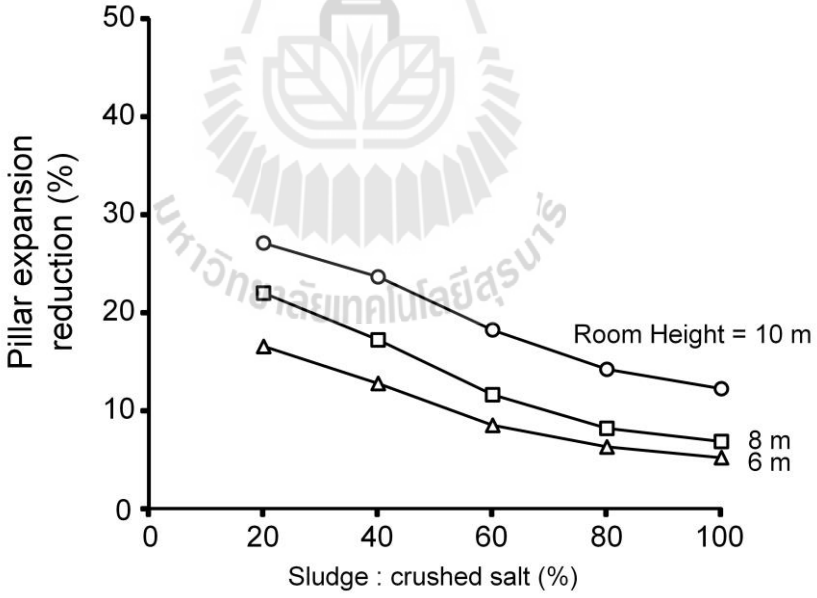

Figure 5.23 pillar expansion reduction as a function of sludge content.

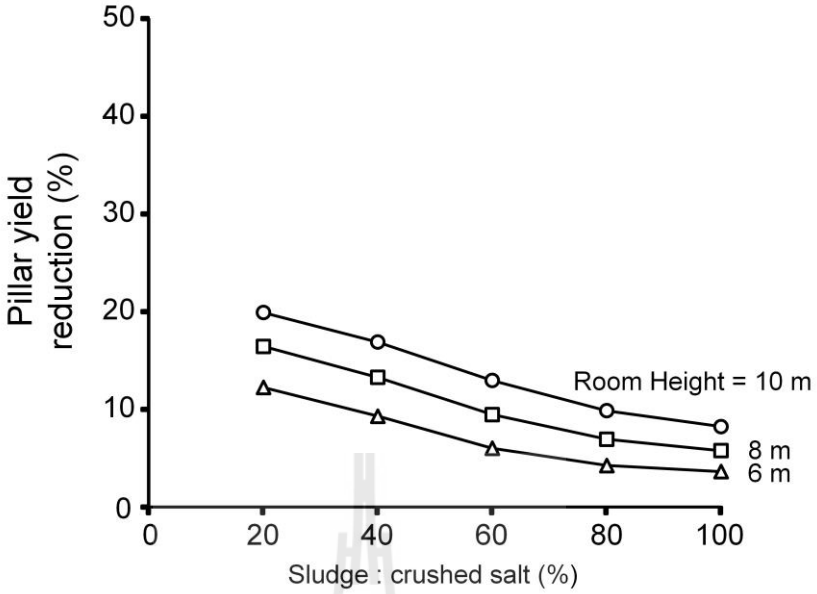

Figure 5.24 Pillar yield reduction as a function of sludge content.

5.4 Discussion

The results obtained from the computer simulations show the ground surface deformation under various opening depths and height. Room and pillar deformations increase with increasing overburden thickness and opening height. This is due to in-situ stress increases with increasing overburden thickness (Newman and Zipf, 2005; Liu, 2011) and hence increase the pillar expansion. The opening height has an effect on pillar shape, slender pillars are more sensitive to deformation more than wider pillars (Dolinar and Esterhuizen, 2007; Malan, 2012; Porathur et al., 2013). These result in the roof collapsed, and hence the surface subside occurred. Figures 5.20 through 5.24 show the reduction of surface subsidence and room and pillar deformation. The result clearly show that the compacted sludge-crushed salt mixture can reduce the deformation of surface, room and pillar, especially when room height is very high. The sludge to crushed salt 20:80 ratio is probably the best ratio for backfill in this study. This is because ratio gives the maximum

mechanical properties (density, elastic modulus, Poisson's ratio, cohesion) for supporting the room and pillar.

CHAPTER VI

DISCUSIONS, CONCLUSIONS AND RECOMMENDATIONS FOR FUTURE STUDIES

6.1 Discussions

This section discusses the results of the study of the effects of sludge-crushed salt ratios on the mechanical and hydraulic properties for use in salt mine. Comparison of the results and findings from this study with those obtained elsewhere under similar test conditions have also been made.

The shear strength of the mixtures increases with decreasing of sludge contents. This is because the effect of crushed salt particles with large grain sizes shows greater interlocking behavior between the particles (Lambe and Whitman, 1969). The result agrees with those of Sonsakul and Fuenkajorn (2013) who studied the shear strength of compacted bentonite-crushed salt mixtures. They find that larger shear strengths are obtained for the mixtures with higher amounts and particle sizes of crushed salt.

The higher sludge content decreases the permeability of the mixtures. This is because the particle sizes of sludge is very small, it can fill and reduce void between crushed salt grains, and hence the fluid flows through the mixture with lower velocity. The result agrees with Shor et al. (1981) who study the relationship between permeability, porosity with the initial grain size by consolidation mixture between of crushed salt and brine. They find that the fine grains (0.02 cm) can reduce porosity

and permeability better than coarse grains (0.34 cm). These observations agree well with Akgün et al. (2015) and Sonsakul et al. (2013) who study the mechanical and hydraulic performance of compacted bentonite-sand for use in underground waste disposal repositories. The results show that the permeability decreases with increasing bentonite content.

The shear strength parameters and permeability properties are the main factors for sealing design to minimize brine leakage in salt mine. The performance of compacted sludge-crushed salt as a sealing material are compared with bentonite-crushed salt (Sonsakul et al., 2013), as shown in Table 6.1.

The sludge can substitute the bentonite due to the similarity of mechanical and hydraulic properties. A comparison between the properties of sludge (Bumrungsuk., 2015) and bentonite (Daeman and Ran, 1996) is summarized in Table 6.2.

The results obtained from the computer simulations clearly show the effectiveness of compacted sludge-crushed salt mixtures. They can reduce the pillar expansion which is related to the surface subsidence. This agrees with Tesarik et al. (2003) who study post-failure behavior of pillar after backfill, they found that the backfill induces confining pressure on pillar and limits pillar dilation, and hence it can support more load than unconfined pillar (without backfill).

6.2 Conclusions

The sludge used in this study obtained from the Metropolitan Waterworks Authority and has the grain size ranging from 0.001 to 0.475 mm. The main mineral composition is silica. The basic properties of sludge including: liquid limit = 59%, plastic limit = 31%, plastic index = 28% and specific gravity = 2.56.

Table 6.1 Comparison of properties between sludge-crushed salt and bentonite-crushed salt mixtures.

Properties	Sludge-crushed salt	Bentonite-crushed salt (Sonsakul et al., 2013)
Dry density (g/cm^3)	1.3-1.8	1.8
Permeability (m^2)	10^{-13} - 10^{-17}	10^{-12} - 10^{-19}
Cohesion (MPa)	0.07-0.18	0.15-0.28
Friction angle (degrees)	27-42	9-36
Optimum brine content (%)	4-34	8-20

Table 6.2 Comparison of properties between sludge and bentonite.

Properties	Material Properties	
	Sludge (Bumrungsuk, 2015)	Bentonite (Daeman and Ran, 1996)
Composition	Silica 90%	Monmorillonite 90%
Liquid Limit	59	105
Plastic Limit	31	35
Density (g/cm^3)	1.8-2.0	1.8
Permeability (m^2)	Less than 10^{-11}	Less than 10^{-16}
Uniaxial compressive strengths (MPa)	2.0-7.0	2.9-5.0
Swell pressure (MPa)	-	1-2
Brine content (%)	5	4

The sludge sample is classified according to the Unified Soil Classification System as inorganic silt (MH).

Crushed salt has been obtained from the Lower Member of the Maha Sarakham Formation. The grain sizes of crushed salt range from 0.075 to 2.35 mm.

The maximum dry density and shear strength of sludge-crushed salt mixture is 1.78 ton/m^3 for 10% sludge by weight, and decreases with increasing of sludge content.

The lowest shear strength is observed for sludge content of 100% by weight with the friction angle = 27 degrees and the cohesion = 72 kPa. The highest shear strength is obtained from sludge content of 10% with the friction angle = 42 degrees and the cohesion = 180 kPa.

The permeability of compacted mixtures increases with decreasing of sludge content and which ranges from 10^{-13} to 10^{-17} m^2.

The results of computer simulations are evaluated in terms of the effectiveness of backfill for 50 years by varying the sludge contents of 20, 40, 60, 80 and 100 % by weight. The results clearly show that the deformation of surface subsidence, roof, floor and pillar increase with increasing overburden thickness, opening height and duration before backfilling. The lowest subsidence is observed for 20% sludge content which is from 12.2 to 25.3 cm, and the higher subsidence is observed for 100% sludge content which is ranging from 14.0 to 29.7 cm.

6.3 Recommendations for futures studies

The test results for the sludge-crushed salt mixture have been limited by testing time. To confirm the conclusions drawn in this research, more testing is required as follows:

- More testing should be conducted on crushed salt mixed with different soils or geologic materials.

- Testing time should be longer (months or years) for long-term performance assessment.
- Uniaxial and triaxial compressive strengths of the mixtures should be determined.
- A variety of crushed salt particle sizes should be tested.

REFERENCES

Akgün, H., Ada, M. and Koçkar, M.K. (2015) Performance assessment of a bentonite–sand mixture for nuclear waste isolation at the potential Akkuyu Nuclear Waste Disposal Site, southern Turkey. **Environmental Earth Sciences** 73(10): 6101-6116.

ASTM D1557-09. Standard test method for laboratory compaction characteristics of soil using modified effort. **In Annual Book of ASTM Standards.** 04.08. Philadelphia: American Society for Testing and Materials.

ASTM D5607-95. Standard test method for performing laboratory direct shear strength test of rock specimens under constant normal force. **In Annual Book of ASTM Standards**, 04.08. American Society for Testing and Materials, Philadelphia.

ASTM D422-07. Standard Test Method for Particle-Size Analysis of Soils. Annual Book of ASTM Standards, 04.08, American Society for Testing and Materials, Philadelphia.

ASTM D5856-15. Standard Test Method for Measurement of Hydraulic Conductivity of Porous Material Using a Rigid-Wall, Compaction-Mold Permeameter. In **Annual Book of ASTM Standards**, 04.08, American Society for Testing and Materials, Philadelphia.

ASTM Standard D698–07. Standard Test Method for Laboratory Compaction Characteristics of Soil Using Standard Effort. **Annual Book of ASTM**

Standards, 04.08. American Society for Testing and Materials, West Conshohocken, PA.

Bumrungsuk, A. and Fuenkajorn, K. (2015). Mechanical and Hydraulic Properties of Sludge-Crushed Salt Mixture as Applied for Backfill Material in Salt and Potash Mines. In **The 9th South East Asian Technical University Consortium (SEATUC)**, Suranaree University of Technology, Surasammanakarn. July 27-30, 2015.

Butcher, B.M. (1991). The advantages of a salt/bentonite backfill for Waste isolation pilot plant disposal rooms (Contractor Report SAND90-3074). **Sandia National Laboratories**, Albuquerque, NM.

Case, J.B. and Kelsall, P. (1987). Laboratory investigation of crushes salt consolidation**. International Journal of Rock Mechanics and Mining Science & Geomechanics Abstracts 25** (5): 216-223.

Crosby, K. (2007). Integration of rock mechanics and geology when designing the Udon South sylvinite mine. In **Proceedings of the First Thailand Symposium on Rock Mechanics** (pp. 3-22)**.** Nakhon Patchasima.

Daemen, J.J.K. and Ran, C. (1996). Bentonite as a Waste Isolation Pilot Plant Shaft Sealing Material. Contractor Report SAND96-1968. **Sandia National Laboratories**, Albuquerque, NM.

Das, B. M. (2008). **Introduction to Geotechnical Engineering**. Ontario Canada: Thomson. pp.110-115.

Dolinar, D.R. and Esterhuizen, G.S. (2007). Evaluation of the Effects of Length on Strength of Slender Pillars in Limestone Mines Using Numerical Modeling. In

Proceedings of the 26th International Conference on Ground Control in Mining (304-313). Morgantown, West Virginia

Fuenkajorn, K. (2007). Design process for sealing of boreholes in rock mass. In **Proceedings of the First Thailand Symposium on Rock Mechanics**, September, 13-14, Khao Yai, Thailand, Published by Geomechanics Research Unit, Suranaree University of Technology, Nakhon Ratchasima, Thailand, pp. 245-252.

Fuenkajorn, K., and Daemen, J.J.K. (1987). Mechanical interaction between rock and multi-component shaft or borehole plugs: Rock mechanics. In I. W. Farmer, J. J. K. Daemen, C. S. Desai, C. E. Glass, and S. P. Neuman (eds.). **Rock Mechanics Proceedings of the 28th U.S. Symposium** (pp. 165-172). Rotterdam: A.A. Balkema.

Fuenkajorn, K. and Daemen, J.J.K. (Eds.), 1996. **Sealing of Boreholes and Underground Excavations in Rock**. Chapman and Hall, London.

Gullu, H. and Girisken, S., (2013). Performance of fine-grained soil treated with industrial wastewater sludge**. Environmental Earth Sciences. 70:777-788.**

Hansen, F. D. (1997). Reconsolidating salt: compaction constitutive modeling, and physical processes. **International Journal of Rock Mechanics and Mining Sciences** 34 (3-4), paper No. 119.

Japakasetr, T. and Suwanich, P. (1977). Potash and rock salt in Thailand Bangkok: Economic Geology Division. **Department of Mineral Resources**. Bangkok.

Japaksetr, T. (1985). Review on rock salt and potash exploration in Northeast Thailand. In **Proceedings Conference on Geology and Mineral Resources**

Development of the Northeast of Thailand (pp. 135-147)**.** Khon Kaen University, Thailand.

Kelsall, P.C., Case, J.B., Coons, W.E., Franzone, J.G. and Meyer, D. (1984). Schematic designs for penetration seals for a repository in the Permian basin. WMI/ONWI-564, prepared by IT Corporation for office of Nuclear Waste Isolation. **Battelle Memorial Institute**. Columbus, Ohio.

Lambe, T.W. and Whitman, R.V. (1969). **Soil Mechanics**. John Wiley&Sons Ltd., Chichester. 553 p.

Liu, C. (2011). Distribution laws of in-situ stress in deep underground coal mines. In **Proceedings conference on First International Symposium on Mine Safety Science and Engineering** (pp. 909-917). Beijing, China.

Malan, D.F. (2012). Pillar Design in the Hard Rock Mines of South Africa. **International Journal of Mining and Geo-Engineering.** (vol 46, pp. 163-191)**.**

Newman, N. and Zipf, R.K. (2005). Analysis of Highwall Mining Stability - The Effect of Multiple Seams and Prior Auger Mining on Design. In **Proceedings of the 24th International Conference on Ground Control in Mining** (pp. 208-217)**.** Morgantown, West Virginia.

Porathur, J.L., Karekal, S. and Palroy, P. (2013). Web pillar design approach for Highwall Mining extraction. **International Journal of Rock Mechanics and Mining Sciences.** 64: 73-83.

Pusch, R. (1983). Borehole sealing for underground waste storage. **ASCE Journal of Geotechnical Engineering**. 109: 113–119.

Ran, C., Daemen, J. J. K., Schuhen, M. D. and Hansen, F. D. (1997). Dynamic compaction properties of bentonite. **International Journal of Rock Mechanics and Mining Sciences.** 34(3-4): 253.e1-253.e19.

Samsri, P., Sriapai, T., Walsri, C. and Fuenkajorn, K. (2010). Polyaxial creep testing of rock salt. In **Proceedings of the Third Thailand Symposium on Rock Mechanicson** (pp. 125-132). Thailand.

Shor, A.J., Baes, C.F. and Canonico, C.M. (1981). Consolidation and permeability of salt in brine (ORNL-5774). **The Oak Ridge National Laboratory for the U.S. Department of Energy**. Oak Ridge, TN.

Sriapai. T., Chaowarin, W. and Fuenkajorn, K. (2012). Effects of temperature on compressive and tensile strengths of salt. **Science Asia.** 38: 166-174.

Sonsakul, P., Walsri, C. and Fuenkajorn, K., **Shear strength and permeability of compacted bentonite-crushed salt seals**. In Proceedings of the Fourth Thailand Symposium on Rock Mechanics, January 24-25, 2013, Wang Nam Keaw, Nakhon Ratchasima, Thailand, Published by Geomechanics Research Unit, Suranaree University of Technology, Nakhon Ratchasima, pp. 99-109, 2013.

Suwanich, P. and Ratanajaruraks, P. (1986). Sequences of rock salt and potash in Thailand (Nonmetallic Minerals Bulletin No. 1). Bangkok: Economic Geology, Division. **Department of Mineral Resources**. Bangkok.

Suwanich, P., Ratanajaruraks, P. and Kunawat, P. (1982). Core log Bamnet Narong area at Chaiyaphum province. Bangkok: Economic Geology Division. **Department of Mineral Resources.** Bangkok**.**

Tesarik, D.R., Seymour, J.B. and Yanske, T.R. (2003) Post-failure behavior of two mine pillars confined with backfill. **International Journal of Rock Mechanics and Mining Sciences.** 64: 73-83.

Wetchasat, K. and Fuenkajorn, K., (2013). **Laboratory Assessment of Mechanical and Hydraulic Performance of Sludge-Mixed Cement Grout in Rock Fractures.** In Proceedings of the Fourth Thailand Symposium on Rock Mechanics, January 24-25, 2013, Wang Nam Keaw, Nakhon Ratchasima, Thailand, Published by Geomechanics Research Unit, Suranaree University of Technology, Nakhon Ratchasima, pp. 259-268.

APPENDIX A

CONSTANT HEAD FLOW TEST RESULTS

Table A.2 Hydraulic conductivity (m/s), of sludge-crushed salt mixtures.

Days	S:C ratio				
	10:90	**30:70**	**50:50**	**70:30**	**100:0**
1	2.79×10^{-6}	3.86×10^{-7}	8.39×10^{-8}	4.95×10^{-9}	4.02×10^{-10}
2	3.43×10^{-6}	4.21×10^{-7}	4.83×10^{-8}	5.14×10^{-9}	4.08×10^{-10}
3	2.36×10^{-6}	3.86×10^{-7}	4.95×10^{-8}	4.76×10^{-9}	4.02×10^{-10}
4	3.00×10^{-6}	3.86×10^{-7}	4.93×10^{-8}	5.36×10^{-9}	4.36×10^{-10}
5	3.86×10^{-6}	4.21×10^{-7}	5.97×10^{-8}	5.59×10^{-9}	4.68×10^{-10}
6	3.22×10^{-6}	3.86×10^{-7}	4.50×10^{-8}	5.85×10^{-9}	5.14×10^{-10}
7	3.43×10^{-6}	4.21×10^{-7}	5.01×10^{-8}	6.43×10^{-9}	5.36×10^{-10}
8	3.43×10^{-6}	4.63×10^{-7}	7.50×10^{-8}	6.12×10^{-9}	5.25×10^{-10}
9	3.00×10^{-6}	3.86×10^{-7}	5.09×10^{-8}	5.85×10^{-9}	5.47×10^{-10}
10	5.14×10^{-6}	4.21×10^{-7}	5.73×10^{-8}	6.20×10^{-9}	5.59×10^{-10}
11	2.79×10^{-6}	3.86×10^{-7}	5.63×10^{-8}	5.83×10^{-9}	5.25×10^{-10}
12	3.22×10^{-6}	4.21×10^{-7}	5.00×10^{-8}	4.95×10^{-9}	4.95×10^{-10}
13	3.00×10^{-6}	3.86×10^{-7}	4.36×10^{-8}	4.93×10^{-9}	4.36×10^{-10}
14	3.43×10^{-6}	3.86×10^{-7}	5.50×10^{-8}	5.97×10^{-9}	5.40×10^{-10}
15	3.00×10^{-6}	4.21×10^{-7}	5.69×10^{-8}	4.50×10^{-9}	5.01×10^{-10}
16	3.43×10^{-6}	3.86×10^{-7}	6.66×10^{-8}	5.01×10^{-9}	4.72×10^{-10}
17	3.43×10^{-6}	4.21×10^{-7}	5.96×10^{-8}	7.50×10^{-9}	4.01×10^{-10}
18	3.86×10^{-6}	3.86×10^{-7}	5.87×10^{-8}	5.09×10^{-9}	4.05×10^{-10}
19	3.43×10^{-6}	4.21×10^{-7}	5.96×10^{-8}	5.73×10^{-9}	4.32×10^{-10}
20	3.43×10^{-6}	4.21×10^{-7}	6.01×10^{-8}	5.63×10^{-9}	5.56×10^{-10}
21	3.86×10^{-6}	3.86×10^{-7}	5.78×10^{-8}	5.00×10^{-9}	5.48×10^{-10}
22	2.79×10^{-6}	4.21×10^{-7}	5.68×10^{-8}	4.36×10^{-9}	5.55×10^{-10}
23	3.43×10^{-6}	3.86×10^{-7}	5.66×10^{-8}	5.50×10^{-9}	4.15×10^{-10}
24	2.36×10^{-6}	3.86×10^{-7}	5.78×10^{-8}	5.69×10^{-9}	4.08×10^{-10}
25	3.00×10^{-6}	4.21×10^{-7}	5.96×10^{-8}	6.66×10^{-9}	4.07×10^{-10}
26	3.86×10^{-6}	3.86×10^{-7}	5.74×10^{-8}	5.96×10^{-9}	4.11×10^{-10}
27	3.22×10^{-6}	4.21×10^{-7}	5.66×10^{-8}	5.87×10^{-9}	5.23×10^{-10}
28	3.43×10^{-6}	4.21×10^{-7}	5.42×10^{-8}	5.96×10^{-9}	5.15×10^{-10}
29	3.43×10^{-6}	3.86×10^{-7}	5.32×10^{-8}	6.01×10^{-9}	4.01×10^{-10}
30	3.00×10^{-6}	4.21×10^{-7}	5.77×10^{-8}	5.78×10^{-9}	4.54×10^{-10}

Table A.1 Constant head flow test results of sludge-crushed salt mixtures.

Days	S:C=10:90		S:C=30:70		S:C=50:50		S:C=70:30		S:C=100:0	
	$V(m^3)$	t(s)	$V(m^3)$	$t(s)$	$V(m^3)$	$t(s)$	$V(m^3)$	$t(s)$	$V(m^3)$	$t(s)$
1	1.63×10^{-6}	9	8.00×10^{-7}	32	9.10×10^{-6}	1673	2.02×10^{-6}	6300	2.55×10^{-7}	9780
2	1.56×10^{-6}	7	1.67×10^{-6}	60	4.50×10^{-6}	1438	2.14×10^{-6}	6420	2.43×10^{-7}	9180
3	1.53×10^{-6}	10	1.65×10^{-6}	66	4.50×10^{-6}	1403	1.92×10^{-6}	6240	2.19×10^{-7}	8400
4	1.56×10^{-6}	8	1.60×10^{-6}	64	4.50×10^{-6}	1409	2.18×10^{-6}	6280	2.39×10^{-7}	8460
5	1.50×10^{-6}	6	1.75×10^{-6}	64	4.50×10^{-6}	1163	1.88×10^{-6}	5200	2.93×10^{-7}	9660
6	1.67×10^{-6}	8	1.70×10^{-6}	68	4.86×10^{-6}	1668	2.73×10^{-6}	7200	2.78×10^{-7}	8340
7	1.56×10^{-6}	7	1.64×10^{-6}	60	5.01×10^{-6}	1543	2.57×10^{-6}	6180	2.60×10^{-7}	7500
8	1.56×10^{-6}	7	1.80×10^{-6}	60	9.00×10^{-6}	1852	2.43×10^{-6}	6120	2.53×10^{-7}	7440
9	1.56×10^{-6}	8	1.85×10^{-6}	74	1.50×10^{-6}	1364	2.00×10^{-6}	5280	3.30×10^{-7}	9300
10	1.67×10^{-6}	5	1.91×10^{-6}	70	5.29×10^{-6}	1424	2.08×10^{-6}	5180	3.13×10^{-7}	8640
11	1.63×10^{-6}	9	1.83×10^{-6}	73	5.35×10^{-6}	1467	2.02×10^{-6}	5340	5.25×10^{-7}	9420
12	1.67×10^{-6}	8	1.91×10^{-6}	70	5.76×10^{-6}	1778	2.02×10^{-6}	6300	4.95×10^{-7}	9600
13	1.56×10^{-6}	8	1.70×10^{-6}	68	4.50×10^{-6}	1593	2.17×10^{-6}	6780	2.64×10^{-7}	9360
14	1.56×10^{-6}	7	1.80×10^{-6}	72	5.50×10^{-6}	1525	2.53×10^{-6}	6540	3.46×10^{-7}	9900
15	1.56×10^{-6}	8	1.88×10^{-6}	69	5.44×10^{-6}	1220	1.45×10^{-6}	4980	2.77×10^{-7}	8520
16	1.56×10^{-6}	7	1.75×10^{-6}	70	5.55×10^{-6}	1285	2.01×10^{-6}	6180	2.64×10^{-7}	8640
17	1.56×10^{-6}	7	1.91×10^{-6}	70	5.14×10^{-6}	1331	3.15×10^{-6}	6480	2.32×10^{-7}	8940
18	1.50×10^{-6}	6	1.83×10^{-6}	73	7.10×10^{-6}	1866	2.10×10^{-6}	6360	2.41×10^{-7}	9180
19	1.56×10^{-6}	7	9.69×10^{-7}	74	5.14×10^{-6}	1330	2.94×10^{-6}	7920	2.10×10^{-7}	7500
20	1.56×10^{-6}	7	1.94×10^{-6}	71	5.11×10^{-6}	1311	2.41×10^{-6}	6600	3.11×10^{-7}	8640
21	1.50×10^{-6}	6	1.73×10^{-6}	69	4.50×10^{-6}	1202	1.56×10^{-6}	4800	2.98×10^{-7}	8400
22	1.08×10^{-6}	6	1.80×10^{-6}	66	4.50×10^{-6}	1223	1.64×10^{-6}	5800	3.00×10^{-7}	8340
23	1.11×10^{-6}	5	1.90×10^{-6}	76	4.86×10^{-6}	1326	2.37×10^{-6}	6600	2.52×10^{-7}	9360
24	9.18×10^{-7}	6	2.03×10^{-6}	81	5.25×10^{-6}	1403	2.01×10^{-6}	5460	2.46×10^{-7}	9300
25	1.36×10^{-6}	7	2.21×10^{-6}	81	5.14×10^{-6}	1330	2.74×10^{-6}	6360	2.61×10^{-7}	9900
26	1.50×10^{-6}	6	1.90×10^{-6}	76	5.28×10^{-6}	1419	2.47×10^{-6}	6400	2.57×10^{-7}	9660
27	1.88×10^{-6}	9	2.13×10^{-6}	78	5.66×10^{-6}	1543	2.71×10^{-6}	7120	2.93×10^{-7}	8640
28	1.78×10^{-6}	8	2.21×10^{-6}	81	5.49×10^{-6}	1562	2.57×10^{-6}	6660	2.80×10^{-7}	8400
29	1.56×10^{-6}	7	1.70×10^{-6}	68	4.50×10^{-6}	1305	2.69×10^{-6}	6900	2.39×10^{-7}	9180
30	1.56×10^{-6}	8	2.13×10^{-6}	78	4.50×10^{-6}	1204	2.56×10^{-6}	6840	2.88×10^{-7}	9780

Table A.3 Intrinsic permeability (m^2), of sludge-crushed salt mixtures.

Days	S:C ratios				
	10:90	**30:70**	**50:50**	**70:30**	**100:0**
1	2.57×10^{-13}	3.56×10^{-14}	7.73×10^{-15}	4.56×10^{-16}	3.70×10^{-17}
2	3.16×10^{-13}	3.88×10^{-14}	4.45×10^{-15}	4.74×10^{-16}	3.76×10^{-17}
3	2.18×10^{-13}	3.56×10^{-14}	4.56×10^{-15}	4.39×10^{-16}	3.70×10^{-17}
4	2.77×10^{-13}	3.56×10^{-14}	4.54×10^{-15}	4.94×10^{-16}	4.02×10^{-17}
5	3.56×10^{-13}	3.88×10^{-14}	5.50×10^{-15}	5.15×10^{-16}	4.31×10^{-17}
6	2.97×10^{-13}	3.56×10^{-14}	4.15×10^{-15}	5.39×10^{-16}	4.74×10^{-17}
7	3.16×10^{-13}	3.88×10^{-14}	4.62×10^{-15}	5.93×10^{-16}	4.94×10^{-17}
8	3.16×10^{-13}	4.27×10^{-14}	6.91×10^{-15}	5.64×10^{-16}	4.84×10^{-17}
9	2.77×10^{-13}	3.56×10^{-14}	4.69×10^{-15}	5.39×10^{-16}	5.04×10^{-17}
10	4.74×10^{-13}	3.88×10^{-14}	5.28×10^{-15}	5.71×10^{-16}	5.15×10^{-17}
11	2.57×10^{-13}	3.56×10^{-14}	5.19×10^{-15}	5.37×10^{-16}	4.84×10^{-17}
12	2.97×10^{-13}	3.88×10^{-14}	4.61×10^{-15}	4.56×10^{-16}	4.56×10^{-17}
13	2.77×10^{-13}	3.56×10^{-14}	4.02×10^{-15}	4.54×10^{-16}	4.02×10^{-17}
14	3.16×10^{-13}	3.56×10^{-14}	5.07×10^{-15}	5.50×10^{-16}	4.98×10^{-17}
15	2.77×10^{-13}	3.88×10^{-14}	5.24×10^{-15}	4.15×10^{-16}	4.62×10^{-17}
16	3.16×10^{-13}	3.56×10^{-14}	6.14×10^{-15}	4.62×10^{-16}	4.35×10^{-17}
17	3.16×10^{-13}	3.88×10^{-14}	5.49×10^{-15}	6.91×10^{-16}	3.70×10^{-17}
18	3.56×10^{-13}	3.56×10^{-14}	5.41×10^{-15}	4.69×10^{-16}	3.73×10^{-17}
19	3.16×10^{-13}	3.88×10^{-14}	5.49×10^{-15}	5.28×10^{-16}	3.98×10^{-17}
20	3.16×10^{-13}	3.88×10^{-14}	5.54×10^{-15}	5.19×10^{-16}	5.12×10^{-17}
21	3.56×10^{-13}	3.56×10^{-14}	5.33×10^{-15}	4.61×10^{-16}	5.05×10^{-17}
22	2.57×10^{-13}	3.88×10^{-14}	5.24×10^{-15}	4.02×10^{-16}	5.12×10^{-17}
23	3.16×10^{-13}	3.56×10^{-14}	5.22×10^{-15}	5.07×10^{-16}	3.82×10^{-17}
24	2.18×10^{-13}	3.56×10^{-14}	5.33×10^{-15}	5.24×10^{-16}	3.76×10^{-17}
25	2.77×10^{-13}	3.88×10^{-14}	5.49×10^{-15}	6.14×10^{-16}	3.75×10^{-17}
26	3.56×10^{-13}	3.56×10^{-14}	5.29×10^{-15}	5.49×10^{-16}	3.79×10^{-17}
27	2.97×10^{-13}	3.88×10^{-14}	5.22×10^{-15}	5.41×10^{-16}	4.82×10^{-17}
28	3.16×10^{-13}	3.88×10^{-14}	5.00×10^{-15}	5.49×10^{-16}	4.75×10^{-17}
29	3.16×10^{-13}	3.56×10^{-14}	4.90×10^{-15}	5.54×10^{-16}	3.70×10^{-17}
30	2.77×10^{-13}	3.88×10^{-14}	5.32×10^{-15}	5.33×10^{-16}	4.18×10^{-17}

BIOGRAPHY

Mr. Pongpoj Sattra was born on April 29, 1991 in Nakhon Ratchasima province, Thailand. He received her Bachelor's Degree in Engineering (Geotechnology) from Suranaree University of Technology in 2013. For his post-graduate, he continued to study with a Master's degree in the Geological Engineering Program, Institute of Engineering, Suranaree university of Technology. During graduation, 2014-2015, he was a part time worker in position of research assistant at the Geomechanics Research Unit, Institute of Engineering, Suranaree University of Technology.